2 Compositions of the Apatite-Group Minerals: Substitution Mechanisms and Controlling Factors

Yuanming Pan

Department of Geological Sciences
University of Saskatchewan
Saskatoon, Saskatchewan S7N 5E2, Canada

Michael E. Fleet

Department of Earth Sciences
University of Western Ontario
London, Ontario N6A 5B7, Canada

INTRODUCTION

The apatite-group minerals of the general formula, $M_{10}(ZO_4)_6X_2$ (M = Ca, Sr, Pb, Na…, Z = P, As, Si, V…, and X = F, OH, Cl…), are remarkably tolerant to structural distortion and chemical substitution, and consequently are extremely diverse in composition (e.g., Kreidler and Hummel 1970; McConnell 1973; Roy et al. 1978; Elliott 1994). Of particular interest is that a number of important geological, environmental/paleoenvironmental, and technological applications of the apatite-group minerals are directly linked to their chemical compositions. It is therefore fundamentally important to understand the substitution mechanisms and other intrinsic and external factors that control the compositional variation in apatites.

The minerals of the apatite group are listed in Table 1, and representative compositions of selected apatite-group minerals are given in Table 2. Also, more than 100 compounds with the apatite structure have been synthesized (Table 3). Phosphate apatites, particularly fluorapatite and hydroxylapatite, are by far the most common in nature and are often synonymous with "apatite(s)". For example, fluorapatite is a ubiquitous accessory phase in igneous, metamorphic, and sedimentary rocks and a major constituent in phosphorites and certain carbonatites and anorthosites (McConnell 1973; Dymek and Owens 2001). Of particular importance in biological systems, hydroxylapatite and fluorapatite (and their carbonate-bearing varieties) are important mineral components of bones, teeth and fossils (McConnell 1973; Wright et al. 1984; Grandjean-Lécuyer et al. 1993; Elliott 1994; Wilson et al. 1999; Suetsugu et al. 2000; Ivanova et al. 2001).

Following Fleischer and Mandarino (1995), Table 1 also includes melanocerite-(Ce), tritomite-(Ce), and tritomite-(Y), the compositions of which correspond closely to synthetic rare-earth borosilicate oxyapatites [e.g., $Ce_{10}(SiO_4)_4(BO_4)_2O_2$, Ito 1968]. These minerals, however, have not been characterized adequately because they are invariably metamict. Hogarth et al. (1973) showed that tritomite-(Ce) and tritomite-(Y), after heating in air for 2 hours at 900°C, recrystallized to britholite-(Ce) and britholite-(Y), respectively, with or without CeO_2 as an additional phase (see also Portnov et al. 1969). Also, it remains unclear whether the compositionally similar melanocerite-(Ce) and tritomite-(Ce) are separate mineral species or not. Other minerals whose structures are closely related to those of apatites include ganomalite (Dunn et al. 1985a), nasonite (Giuseppetti et al. 1971), and samuelsonite (Moore and Araki 1977).

Despite a long history of heated debate and controversy (see McConnell 1973 and Elliott 1994 for reviews), carbonate-bearing apatites with lattice-bound CO_3^{2-} ions are now well established and recognized as the major minerals of phosphorites and the main

Table 1. Summary of the apatite-group minerals

Mineral name	Formula	Space Group	Reference
fluorapatite	$Ca_{10}(PO_4)_6F_2$	$P6_3/m$	Hughes et al. (1989)
hydroxylapatite	$Ca_{10}(PO_4)_6(OH)_2$	$P2_1/b$	Ikoma et al. (1999)
chlorapatite	$Ca_{10}(PO_4)_6Cl_2$	$P2_1/b$	Mackie et al. (1972)
fermorite	$Ca_{10}(PO_4)_3(AsO_4)_3(OH)_2$	$P2_1/m$	Hughes & Drexler (1991)
alforsite	$Ba_{10}(PO_4)_6Cl_2$	$P6_3/m$	Newberry et al. (1981)
pyromorphite	$Pb_{10}(PO_4)_6Cl_2$	$P6_3/m$	Dai & Hughes (1989)
strontium-apatite	$Sr_{10}(PO_4)_6(OH)_2$	$P6_3$	Pushcharovskii et al. (1987)
belovite-(La)	$Sr_6(Na_2La_2)PO_4)_6(OH)_2$	$P\overline{3}$	Pekov et al. (1996)
belovite-(Ce)	$Sr_6(Na_2Ce_2)PO_4)_6(OH)_2$	$P\overline{3}$	Rakovan & Hughes (2000)
deloneite-(Ce)	$NaCa_2SrCe(PO_4)_3F$	$P3$	Khomyakov et al. (1996)
svabite	$Ca_{10}(AsO_4)_3F_2$	$P6_3/m$	Welin (1968)
johnbaumite	$Ca_{10}(AsO_4)_6(OH)_2$	$P6_3/m$	Dunn et al. (1980)
clinomimetite	$Pb_{10}(AsO_4)_6Cl_2$	$P2_1/b$	Dai et al. (1991)
hedyphane	$Pb_6Ca_4(AsO_4)_6Cl_2$	$P6_3/m$	Rouse et al. (1984)
mimetite	$Pb_{10}(AsO_4)_3Cl_2$	$P6_3/m$	Dai et al. (1991)
morelandite	$Ba_{10}(AsO_4)_3Cl_2$	$P6_3/m$ or $P6_3$	Dunn & Rouse (1978)
turneaureite	$Ca_{10}(AsO_4)_3Cl_2$	$P6_3/m$	Dunn et al. (1985b)
britholite-(Ce)	$Ce_6Ca_4(SiO_4)_6(OH)_2$	$P6_3$	Oberti et al. (2001)
britholite-(Y)	$Y_6Ca_4(SiO_4)_6(OH)_2$	$P2_1$	Zhang et al. (1992)
chlorellestadite	$Ca_{10}(SiO_4)_3(SO_3)_3Cl_2$	$P6_3$ or $P6_3/m$	Rouse et al. (1982)
fluorellestadite	$Ca_{10}(SiO_4)_3(SO_3)_3F_2$	$P6_3/m$	Chesnokov et al. (1987)
hydroxylellestadite	$Ca_{10}(SiO_4)_3(SO_3)_3(OH)_2$	$P2_1/m$	Hughes & Drexler (1991)
mattheddleite	$Pb_{10}(SiO_4)_3(SO_4)_3Cl_2$	$P6_3/m$	Steele et al. (2000)
cesanite	$Na_6Ca_4(SO_4)_6(OH)_2$	$P6_3/m$	Deganello (1983)
caracolite	$Na_6Pb_4(SO_4)_6Cl_2$	$P2_1/m$	Schneider (1967)
vanadinite	$Pb_{10}(VO_4)_6Cl_2$	$P6_3/m$	Dai & Hughes (1989)
melanocerite-(Ce)	$Ce_5(Si,B)_3O_{12}(OH,F)\cdot nH_2O$	?	Anovitz & Hemingway (1996)
tritomite-(Ce)	$Ce_5(Si,B)_3(O,OH,F)_{13}$	?	Hogarth et al. (1973)
tritomite-(Y)	$Y_5(Si,B)_3(O,OH,F)_{13}$	?	Hogarth et al. (1973)

components of bones and teeth of the vertebrates (e.g., Wallaeys 1952; Bonel and Montel 1964; Elliott 1964; LeGeros 1965; McConnell 1973; Jahnke 1984; McArthur 1985; Elliott 1994; Wilson et al. 1999; Suetsugu et al. 2000; Ivanova et al. 2001). Bonel and Montel (1964), using the structural positions of the CO_3^{2-} ions inferred from infrared (IR) absorption spectra, classified carbonate-bearing apatites into two types: A-type with CO_3^{2-} ions in the *c*-axis anion channels and B-type with CO_3^{2-} ions substituting for tetrahedral PO_4^{3-} groups. "Francolite" and "dahlite" have been used widely in the literature to describe carbonate-bearing fluorapatite and hydroxylapatite, respectively, but are not valid mineral names because CO_3^{2-} ions are not known to be the dominant anion species substituting for tetrahedral groups (or in the *c*-axis anion channels) in natural carbonate-bearing apatites.

This chapter outlines the compositional variations of the apatite-group minerals, with emphasis on the chemical substitutions that appear to be responsible for these variations. We purposely include data from the large number of synthetic apatites, which may or may not

have natural equivalents but are extremely informative in understanding the crystal chemistry of this complex group of minerals. Also, we use the uptake of rare earth elements (REEs) in fluorapatite, hydroxylapatite, and chlorapatite as examples to illustrate some of the important factors that control the compositional variation in apatites. Following the practice in much of the chemical and mineralogical literature, fluorapatite, hydroxylapatite, and chlorapatite are hereafter abbreviated as FAp, OHAp and ClAp, respectively.

CATION AND ANION SUBSTITUTIONS IN APATITES

It is convenient to discuss the chemical substitutions in apatites relative to FAp, which is the most studied mineral and compound of this group and has the ideal $P6_3/m$ structure (e.g., Sudarsanan et al. 1972; Hughes et al. 1989). The structures of many natural and synthetic apatites deviate from the $P6_3/m$ structure (e.g., Mackie et al. 1972; Hughes et al. 1990; 1992; 1993; Hughes and Drexler 1991; Huang and Sleight 1993; Takahashi et al. 1998; Ikoma et al. 1999; Fleet et al. 2000a,b; Rakovan and Hughes 2000), but these deviations are generally very small. It is reasonable, therefore, to discuss the atomic arrangements of all apatites relative to the hexagonal unit cell and the $P6_3/m$ structure to facilitate direct comparisons among them (e.g., Hughes et al. 1990; Fleet et al. 2000a,b).

Notes for Table 2 (from the next three pages).

1: fluorapatite, Corro de Mercado mine, Durango, Mexico (Young et al. 1969)
2: REE-rich fluorapatite, Pajarito, Otero County, New Mexico, USA (Roeder et al. 1987; Hughes et al. 1991b)
3: Sr-rich fluorapatite, Lovozero massif, Kola Peninsula, Russia (Rakovan & Hughes 2000)
4: carbonate-bearing fluorapatite ("francolite"), Staffel, Germany (Brophy & Nash 1968)
5: hydroxylapatite, Holly Springs, Georgia, USA (Mitchell et al. 1943; a, including 0.15 wt % insoluble)
6: carbonate-bearing hydroxylapatite ("dahllite"), Allendorf, Saxony, Germany (Brophy & Nash 1968)
7: REE-bearing hydroxylapatite in kalsilite-bearing leucitite, Grotta del Cervo, Abruzzi, Italy (Comodi et al. 1999)
8: chlorapatite, Bob's Lake, Ontario, Canada (Hounslow & Chao 1970; b, unit-cell parameters from powder XRD)
9: fermorite, Sitipar deposit, Chhinwara district, India (Smith & Prior 1911; Hughes & Drexler 1991)
10: alforsite, Big Creek, California, USA (Newberry et al. 1981)
11: strontium-apatite, Inagli massif, Aldan, Yakutia, Russia (Efimov et al. 1962)
12: belovite-(La), Mt. Kukisvumchorr, Kola Peninsula, Russia (Pekov et al. 1996)
13: belovite-(Ce), Durango, Mexico (Rakovan & Hughes 2000)
14: deloneite-(Ce), Mt. Koashva, Kola Peninsula, Russia (Khomyakov et al. 1996)
15: svabite, Jakobsberg, Sweden (Welin 1968)
16: johnbaumite, Franklin, New Jersey, USA (Dunn et al. 1980)
17: hedyphane, Långban, Sweden (Rouse et al. 1984)
18: clinomimetite, Johanngeorgenstadt, Germany (Dai et al. (1991)
19: morelandite, Jakobsberg, Sweden (Dunn & Rouse 1978)
20: turneaureite, Långban, Sweden (Dunn et al. 1985b).
21: britholite-(Ce),Vico volcanic complex, Capranica, Latium, Italy (Oberti et al. 2001; c, including 2.12 wt % UO$_2$)
22: britholite-(Y), Henan, China (Zhang et al. 1992)
23: fluorellestadite, Kopeysk, Chelyabinsk basin, south Ural Mountains, Russia (Chesnokov et al. 1987)
24: hydroxylellestadite, Chichibu mine, Saitama Prefecture, Japan (Harada et al. 1971; d, including 0.72 wt % H$_2$O⁻)
25: cesanite from Cesano geothermal field, Latium, Italy (Cavaretta et al. 1981)
26: melanocerite, Burpala alkalic intrusion, north Baikal region, Russia (Portnov et al. 1969; e, total rare earth oxides; f, including 0.63 wt % TiO$_2$ and 0.17% UO$_2$; g, unit-cell parameters obtained after heating at 670ºC)

Table 2. Representative compositions and unit-cell parameters of selected apatite-group minerals.

Analysis	1	2	3	4	5	6	7	8
(wt %)								
P_2O_5	40.78	36.55	39.15	40.33	42.05	39.39	34.22	41.20
As_2O_5	0.10	0.003						
V_2O_5	0.01							
B_2O_3								
SO_3	0.37						1.53	
SiO_2	0.34	1.71					3.11	
Al_2O_3	0.07							
Fe_2O_3	0.06							
FeO		0.169					0.04	
CaO	54.02	38.35	47.14	51.42	55.84	51.58	54.61	53.40
MgO	0.01			1.35	0.10	1.16		
MnO	0.01	0.065			0.07			
PbO								
BaO		0.200						
SrO	0.07	2.63	10.67				1. 57	
Na_2O	0.23	0.01		1.17		0.80		
K_2O	0.01	0.01		0.38				
Y_2O_3	0.097	0.306					0.86	
La_2O_3	0.493	4.48					1.58	
Ce_2O_3	0.551	8.50						
Pr_2O_3	0.094	0.93					0.48	
Nd_2O_3	0.233	3.69						
Sm_2O_3	0.035	0.50						
Eu_2O_3	0.002	<0.059						
Gd_2O_3	0.023	0.33						
Tb_2O_3	0.012	0.477						
Dy_2O_3	0.017	<0.033						
Ho_2O_3	0.003	<0.082						
Er_2O_3	0.011	<0.024						
Tm_2O_3	0.001	<0.005						
Yb_2O_3	0.006	<0.017						
Lu_2O_3	0.001	<0.015						
ThO_2	0.02							
CO_2	0.05			2.70		3.51		
H_2O	0.01			0.63	1.86	1.48	1.10	0.09
F	3.53	3.65	3.37	3.89	0.16	0.44	1.46	0.13
Cl	0.41	0.01		trace	trace	trace	0.02	6.20
-O=F,Cl	1.58		1.42	1.64	0.07	0.19	0.61	1.45
Total	99.94	101.11	98.91	100.23	100.16[a]	98.17	99.92	99.57
a (Å)	9.391(1*	9.406(3	9.416(1)	9.346	9.4166	9.419	9.4035	9.606(4[b]
b		9.405(2						
c	6.878(2	6.913(2	6.924(1)	6.887	6.8745	6.886	6.8990	6.785(3
α (°)		90.02(2						
β		89.98(3						
γ		120.00(2						

* Small number [e.g., (3] following unit cell parameters is 1σ error in the last decimal place.

Table 2 (continued)

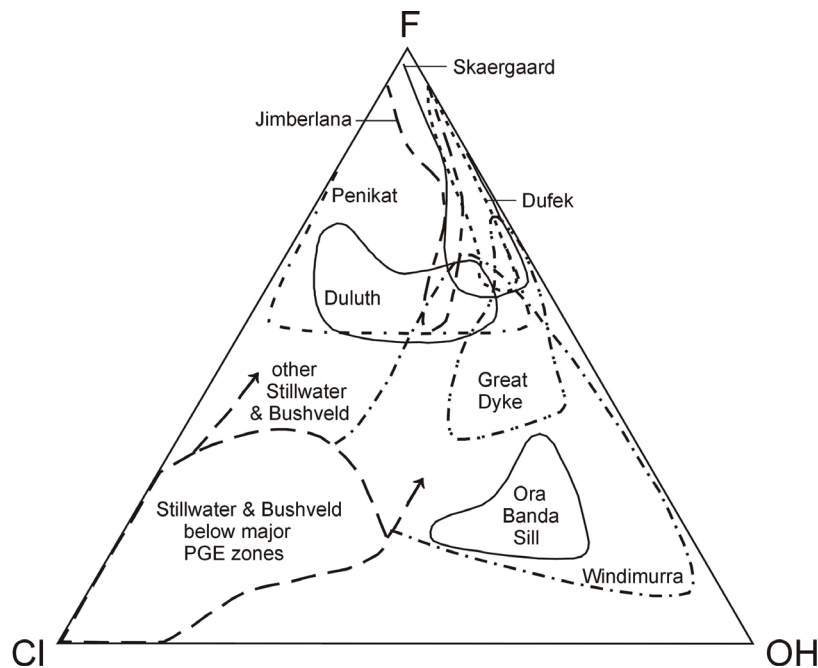| 9	10	11	12	13	14	15	16	17
20.11	22.7	30.44	28.30	27.5	30.71	0.38	1.7	0.4
25.23						51.05	52.2	28.2
		0	0.03			0.69		
	0.1	0.90	0.24	0.9	0.74			
		0.40				0.08		
		0.15						
							0.2	10.3
44.34		10.80	0.50	0.61	14.77	42.07	43.5	
		1.64				0.52	0.1	
	<0.1	0				0.26		
	0.8					3.02		58.0
	67.7	2.70	2.35	2.15	0.10			0.1
9.93	2.7	46.06	40.09	38.1	18.19			1.0
		0.64	4.09	4.19	4.45	0.56		
		0.10			0.07	0.30		
			0.01		0.02			
		0.98	13.08	6.67	8.12			
		2.02	8.15	12.47	13.14			
		0.19	0.30	3.74	1.13			
		0.50	0.30		3.81			
		0.02	0.03		0.34			
		0.004						
		0.011	0.01					
		0.002						
		0.002						
		0.005						
			0.43		0.02			
trace		0.61	0.22	0.01	0.38	0.25	1.3	
0.83	0.7	1.67	2.04	2.39	2.03	1.99	0.2	
0.08	3.6			0.03		0.12	0.1	3.3
0.35	1.2	0.70	0.86	1.01	0.85	0.87	0.1	0.7
100.17	101.7	99.74	99.31	97.86	97.18	100.42	99.2	100.6
9.594(2*	10.284(	9.66(1	9.647(1	9.659(2	9.51(1	9.75	9.70(2	10.140(3
9.597(2	2							
6.975(3	7.651(3	7.19(1	7.170(1	7.182(2	7.01(1	6.92	6.93(2	7.185(4
90.03(4								
89.95(3								
119.97(1								

* Small number [e.g., (3] following unit cell parameters is 1σ error in the last decimal place.

Table 2 (concluded)

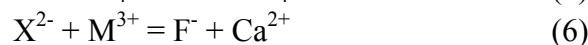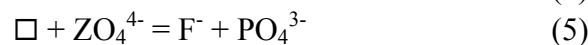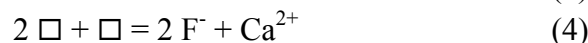| 18	19	20	21	22	23	24	25	26
0.33	2.05	6.1	1.11	0.327	1.31	0.66		2.85
22.05	28.11	44.9						
								4.37
			0.35		20.75	21.56	52.6	
0.14			21.10	25.254	15.3	17.30		14.73
				0.317	1.84	trace		0.93
					1.38	0.21		1.50
	0.41			0.121	0.18			
0.00	8.85	43.8	16.80	13.707	55.0	54.51	18.9	12.66
	0.39	0.0		0		trace		0.59
		1.9	0.18	0.041		0.04		0.12
74.61	24.85	0.7						
	33.00							
			0.00			0.28	0.72	0.48
			0.00	0	0.33	0.34	23.3	
				0.086	0.10	0.07	0.21	
			1.71	44.43				
			11.23					38.89[e]
			21.70	5.957				
			2.19					
			5.92					
			0.72					
			0.06					
			0.50					
			0.31	4.806				
			0.14	2.663				
			0.12					
			11.92	0.399				12.39
					0.66	1.65		
	trace	nd	0.13		0.30	2.76[d]	2.91	2.55
	0.00	1.2	2.12		3.60	0.28	0.25	9.10
2.58	3.69	3.2				0.91	0.44	
0.58	0.83	1.2	0.89			0.32	0.21	3.86
99.28	100.52	100.6	99.54[c]	98.11	100.76	100.25	99.12	100.64[f]
10.189(3*	10.869(2	9.810(4	9.547(4	9.504(5	9.485(2	9.491(1	9.442(4	9.517[g]
20.372(8				9.414(4				
7.46(1	7.315(2	6.868(4	6.991(1	6.922(2	6.916(2	6.921(1	6.903(3	6.989
119.88(3				119.71(4				

* Small number [e.g., (3] following unit cell parameters is 1σ error in the last decimal place.

Substitution for fluorine (X anions)

The X anions in the *c*-axis channels of natural apatites are dominated by F^-, OH^-, and Cl^- (Tables 1 and 2). Additional substituents in the *c*-axis anion channels include other monovalent anions (Br^-, I^-, O_2^-, O_3^-, BO_2^-, NCO^-, NO_3^-, and NO_2^-), divalent anions (O^{2-}, CO_3^{2-}, O_2^{2-}, S^{2-}, NCN^{2-}, and NO_2^{2-}), vacancy ($\square$) and vacancy clusters, and neutral and organic molecules (McConnell 1973; Trombe and Montel 1978; Elliott 1994). Major substitutions responsible for the incorporation of these anions and vacancies into the *c*-axis channels are as follows:

$$X^- = F^- \qquad\qquad (1)$$
$$\square + X^{2-} = 2\ F^- \qquad\qquad (2)$$
$$\square + M^+ = F^- + Ca^{2+} \qquad\qquad (3)$$
$$2\ \square + \square = 2\ F^- + Ca^{2+} \qquad\qquad (4)$$
$$\square + ZO_4^{4-} = F^- + PO_4^{3-} \qquad\qquad (5)$$
$$X^{2-} + M^{3+} = F^- + Ca^{2+} \qquad\qquad (6)$$

Figure 1. Channel anion (X) composition of apatites from a variety of layered intrusions showing extent of solid solution among FAp-OHAp-ClAp end-members. The molar proportion of F, OH and Cl in apatite of near ideal $Ca_{10}(PO_4)_6X_2$ composition appears to be limited only by the composition of these components in coexisting fluid/melt (after Boudreau 1995).

Monovalent anions. Extensive substitutions among F, OH, and Cl have been well documented in natural apatite-group minerals. For example, the compositions of apatites from layered intrusions span almost the complete range of F, OH, and Cl end-members (Fig. 1; Boudreau 1995 and references therein). Also, complete binary (F-OH, F-Cl, and Cl-OH) solid solutions of Ca, Sr, and Pb apatites have been synthesized (e.g., Wallaeys 1952; Prener 1967; Ruszala and Kostiner 1975). These monovalent anions are known to reside mostly in the *c*-axis anion channels but may differ greatly in their precise location owing to significant differences in ionic radius (Mackie et al. 1972; Elliott et al. 1973; Sudarsanan and Young 1980; Hughes et al. 1989, 1990; Fleet et al. 2000a,b; Rakovan and Hughes 2000). The crystal-chemical complexity related to substitutions involving these monovalent anions in calcium phosphate apatites has been discussed in Hughes and Rakovan (this volume).

Table 3. Formulas of selected synthetic compounds with the apatite structure.

Composition	*Reference*
$Ba_{10}(PO_4)_6F_2$	Mathew et al. (1979)
$Ba_{10}(PO_4)_6(OH)_2$	Engel (1973); Fowler (1974)
$Ba_{10}(PO_4)_6Cl_2$	Hata et al. (1979)
$Ba_{10}(PO_4)_6CO_3$	Mohseni-Koutchesfehani (1961)
$Ca_{10}(PO_4)_6Br_2$	Elliott et al. (1981)
$Ca_{10}(PO_4)_6CO_3$	Elliott et al. (1980)
$Ca_{10}(PO_4)_6O\square$	Wallaeys (1952)
$Ca_{10}(PO_4)_6O_2$	Trombe & Montel (1978)
$Ca_{10}(PO_4)_6(NCN)\square$	Trombe & Montel (1981)
$Ca_6Eu_2Na_2(PO_4)_6F_2$	Mayer & Cohen (1983)
$Ca_8Eu_2(PO_4)_6O_2$	Piriou et al. (1987)
$Mn_{10}(PO_4)_6Cl_2$	Klement & Haselbeck (1965)
$Sr_{10}(PO_4)_6F_2$	Kreidler & Hummel (1970)
$Sr_{10}(PO_4)_6Cl_2$	Kingsley et al. (1965)
$Sr_{10}(PO_4)_6CO_3$	Nadal et al. (1971)
$Sr_{10}(PO_4)_6O\square$	Hata et al. (1978)
$Sr_{10}(PO_4)_6O_2$	Trombe & Montel (1978)
$Sr_{9.4}Na_{0.2}\square_{0.4}(PO_4)_6BO_2$	Calvo et al. (1975)
$Cd_{10}(PO_4)_6(OH)_2$	Hata et al. (1978)
$Cd_{10}(PO_4)_6Cl_2$	Wilson et al. (1977)
$Cd_{10}(PO_4)_6Br_2$	Wilson et al. (1977)
$Cd_{10}(PO_4)_6I_2$	Sudarsanan et al. (1977)
$Pb_{10}(PO_4)_6(OH)_2$	Engel (1970)
$Pb_{10}(PO_4)_6O\square$	Wondratschek (1963)
$Pb_{10}(PO_4)_6S\square$	Trombe & Montel (1975)
$Pb_8K_2(PO_4)_6\square_2$	Mathew et al. (1980)
$\square Pb_9(PO_4)_6\square_2$	Hata et al. (1980)
$Bi_2Ca_8(PO_4)_6O_2$	Buvaneswari & Varadaraju (2000)
$La_2Ca_8(PO_4)_6O_2$	Buvaneswari & Varadaraju (2000)
$La_2Sr_8(PO_4)_6O_2$	Lacout & Mikou (1989)
$Ca_{10}(AsO_4)_6CO_3$	Roux & Bonel (1977)
$Sr_{10}(AsO_4)_6(OH)_2$	Mayer et al. (1975)
$Sr_{10}(AsO_4)_6CO_3$	Hitmi et al. (1986)
$Cd_{10}(AsO_4)_6Br_2$	Sudarsanan et al. (1977)
$Cd_{10}(AsO_4)_6I_2$	Sudarsanan et al. (1977)
$Pb_{10}(AsO_4)_6(OH)_2$	Engel (1970)
$Eu_{10}(AsO_4)_6(OH)_2$	Mayer et al. (1975)
$Ca_{10}(VO_4)_6(OH)_2$	Kutoglu (1974)
$Sr_{10}(VO_4)_6(OH)_2$	Mayer et al. (1975)
$Cd_{10}(VO_4)_6Br_2$	Sudarsanan et al. (1977)
$Cd_{10}(VO_4)_6I_2$	Sudarsanan et al. (1977)
$Pb_{10}(VO_4)_6(OH)_2$	Engel (1970)
$Bi_2Ca_8(VO_4)_6O_2$	Huang & Sleight (1993)
$Pb_{9.85}\square_{0.15}(O_4)_6I_{1.7}\square_{0.3}$	Audubert et al. (1999)

Table 3, continued

Composition	*Reference*
$Ca_{10}(CrO_4)_6(OH)_2$	Banks & Jaunarajs (1965)
$Sr_{10}(SiO_4)_3(CrO_4)_3F_2$	Schwarz (1967a)
$K_6Pb_4(CrO_4)_6F_2$	Pascher (1963)
$Na_6Pb_4(SO_4)_6F_2$	Kreidler & Hummel (1970)
$K_6Ca_4(SO_4)_6F_2$	Fayos et al. (1987)
$Na_6Cd_4(SO_4)Cl_2$	Perret & Bouillet (1975)
$Na_6Pb_4(SO_4)_6Cl_2$	Perret & Bouillet (1975)
$Pb_6K_4(PO_4)_4(SeO_4)_2\square_2$	Schwarz (1967a)
$Pb_6K_4(AsO_4)_4(SeO_4)_2\square_2$	Schwarz (1967a)
$Ca_4La_6(SiO_4)_6(OH)_2$	Ito (1968)
$Ba_4La_6(SiO_4)_6(OH)_2$	Ito (1968)
$Sr_4La_8(SiO_4)_6(OH)_2$	Ito (1968)
$Cd_4La_6(SiO_4)_6(OH)_2$	Ito (1968)
$Mg_4La_6(SiO_4)_6(OH)_2$	Ito (1968)
$Pb_4La_6(SiO_4)_6(OH)_2$	Ito (1968)
$Mn_4La_6(SiO_4)_6(OH)_2$	Ito (1968)
$Ca_2La_8(SiO_4)_6O_2$	Ito (1968)
$Ba_2La_8(SiO_4)_6O_2$	Ito (1968)
$Sr_2La_8(SiO_4)_6O_2$	Ito (1968)
$Cd_2La_8(SiO_4)_6O_2$	Ito (1968)
$Mg_2La_8(SiO_4)_6O_2$	Ito (1968)
$Pb_2La_8(SiO_4)_6O_2$	Ito (1968)
$Mn_2La_8(SiO_4)_6O_2$	Ito (1968)
$NaLa_9(SiO_4)_6O_2$	Ito (1968)
$LiY_9(SiO_4)_6O_2$	Ito (1968)
$\square CaLa_8(SiO_4)_6F_2$	Grisafe & Hummel (1970)
$\square_2La_8(SiO_4)_6\square_2$	Grisafe & Hummel (1970)
$Sm_{10}(SiO_4)_4(SiO_3N)_2O_2$	Gaudé et al. (1975)
$Cr_2Sm_8(SiO_4)_4(SiO_3N)_2O_2$	Maunaye et al. (1976)
$Y_{10}(SiO_4)_4(BO_4)_2O_2$	Ito (1968)
$La_{10}(SiO_4)_4(BO_4)_2O_2$	Mazza et al. (2000)
$Sr_{10}(SO_4)_3(GeO_4)_3F_2$	Schwarz (1967b)
$Sr_{10}(PO_4)_4(GeO_4)_2\square_2$	Schwarz (1968)
$Ca_4La_6(GeO_4)_6(OH)_2$	Cockbain & Smith (1967)
$NaLa_9(GeO_4)_6O_2$	Takahashi et al. (1998)
$Ba_{10}(ReO_5)_6Cl_2$	Besse et al. (1979)
$Ba_{10}(ReO_5)_6Br_2$	Baud et al. (1979)
$Ba_{10}(ReO_5)_6CO_3\square$	Baud et al. (1980)
$Ba_{10}(ReO_5)_6(O_2)_2$	Besse et al. (1980)
$Na_6Pb_4(BeF_4)_6F_2$	Engel (1978)

Bromine and I occur only as trace constituents in natural apatites (up to 100 ppm Br, O'Reilly and Griffin 2000; Dong and Pan 2002), although several compounds of BrAp and IAp have been synthesized (e.g., Akhavan-Niaki 1961; Sudarsanan et al. 1977; Baud et al. 1979; Elliott et al. 1981; Audubert et al. 1999). Single-crystal X-ray refinements of synthetic BrAp and IAp revealed that Br^- and I^- ions reside in the c-axis anion channels but, unlike F in FAp, are located at (0,0,0) (Sudarsanan et al. 1977; Wilson et al. 1977; Elliott et al. 1981; Audubert et al. 1999). These positions suggest that Br and I are incompatible for solid solution with F, OH or Cl, which partly explains the paucity of Br and I in natural apatites. Another important reason for the low Br and I contents in apatites is that these elements partition strongly into coexisting solutions/melts (e.g., Böhlke and Irwin 1992; Berndt and Seyfried 1997; Dong and Pan 2002).

Other monovalent anions, such as O_2^-, O_3^-, BO_2^-, NCO^-, NO_3^-, and NO_2^-, have been shown to occur in various synthetic apatites (Calvo et al. 1975; Dugas and Rey 1977; Tochon-Danguy et al. 1978; Trombe and Bonel 1978; Dowker and Elliott 1983; Ito et al. 1988). For example, an electron paramagnetic resonance (EPR) study by Dugas and Rey (1977) detected the presence of superoxide O_2^- ions in synthetic oxygen-rich apatites and suggested the location of the O_2^- ions away from (0,0,1/4) on the basis of an anisotropic Zeeman splitting factor (g). Similarly, Besse et al. (1980) reported that the O_2^- ions in the compound $Ba_{10}(ReO_5)_6(O_2)_2$ are located at (0,0,0.673). Tochon-Danguy et al. (1978) assigned an asymmetrical EPR signal from an OHAp sample excited in an atmosphere of oxygen gas at 80°C and 130 Pa to the presence of O_3^- ions in the c-axis anion channels. Calvo et al. (1975) showed that BO_2^- ions in the apatite anion channels have a linear configuration with the B atom at (0,0,1/2) and O atoms at (0,0,0.3278) and (0,0,0.6722) (see also Ito et al. 1988). Similarly, a polarized IR study of heated enamel by Dowker and Elliott (1983) showed that the NCO^- ion, formed from reaction between NH_4^+ and CO_2 during heating, is highly oriented in the c-axis direction, indicative of a location in the c-axis anion channels. Elliott (1994) suggested that the NCO^- ion may be located at a position similar to that of the BO_2^- ion, although the C atom must be slightly displaced from (0,0,1/2) along the c-axis because of the absence of a center of symmetry in the NCO^- ion. The nitrate (NO_3^-) and nitrite (NO_2^-) ions also have been detected by IR spectroscopy of A-type carbonate-bearing apatite samples heated in nitrogen monoxide and have been suggested to be located in the c-axis anion channels (Dugas et al. 1978).

Vacancy and vacancy clusters. Sudarsanan et al. (1977) and Wilson et al. (1977) showed that vacancies are common in the c-axis anion channels, and apatites with completely vacant anion channels via Substitutions (3), (4), and (5) have been synthesized [for example,

$Pb_8K_2(PO_4)_6\square_2$, Mathew et al. 1980;

$\square Pb_9(PO_4)_6\square_2$, Hata et al. 1980;

$Pb_{10}((PO_4)_4(SiO_4)_2\square_2$, Merker et al. 1970).
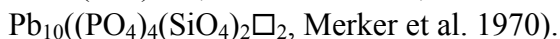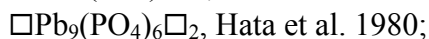
The anion vacancies in CaF_2-, $Ca(OH)_2$-, and $CaCl_2$-deficient apatites are most likely compensated by loss of Ca atoms [i.e., Substitution (4); see also Audubert et al. 1999; Christy et al. 2001]. For example, vacancy clusters of the type $\square_{OH}\square_{Ca2}HPO_4$ have been proposed to occur in synthetic $Ca(OH)_2$-deficient OHAp (Labarthe et al. 1973). Cho and Yesinowski (1993; 1996) detected a lack of coherence in the ···OH OH OH··· chains in OHAp by a multiple-quantum NMR dynamics study on the quasi-one-dimensional distribution of protons and interpreted it to represent OH^- deficiency. Another type of vacancy in the anion channels is related to the incorporation of divalent anions (e.g., O^{2-}, S^{2-}, and CO_3^{2-}) in the channels via Substitution (2). However, $Ca_{10}(PO_4)_6O\square$, an end-member of this substitution, is not stable (Ito 1968) and hydrates readily to oxyhydroxylapatite in air (Trombe and Montel 1978). EPR studies of FAp (Warren 1972) provided evidence for different arrangements of vacancies in the anion channels,

namely: (1) $(O\square)^0$, one vacancy and one O atom replacing two F^- ions; and (2) $(\square O\square)^+$, two vacancies and one O atom substituting for three F^- ions. Wondratschek (1963) reported the loss of the 6_3 axis in $Pb_{10}(PO_4)_6O\square$ and attributed it to an ordered arrangement of vacancy and O^{2-} along the *c*-axis.

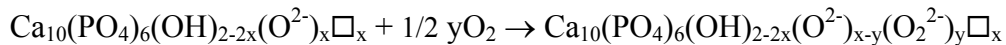*Divalent anions.* Partial or complete replacement of the monovalent ions (F^-, OH^-, or Cl^-) in the *c*-axis channels by various divalent anions (e.g., O^{2-}, CO_3^{2-}, O_2^{2-}, S^{2-}, NCN^{2-}, and NO_2^{2-}) has also been well established. For example, the substitution of O^{2-} for F^- is indicated by the presence of natural oxygen-rich FAp (e.g., Young and Munson 1966; Sudarsanan and Young 1980) and has also been demonstrated by the synthesis of oxyapatites (Ito 1968; Felsche 1972; Schroeder and Mathew 1978; Azimov et al. 1981; Piriou et al. 1987; Lacout and Mikou 1989; Takahashi et al. 1998; Buvaneswari and Varadaraju 2000). Two examples of Substitution (2) are the incorporation of O^{2-} and CO_3^{2-} ions into oxyapatites and A-type carbonate-bearing apatites (see below), respectively. Examples for Substitution (6) will be given in the section on the incorporation of trivalent REEs into apatites.

In synthetic A-type carbonate apatites [e.g., $Ca_{10}(PO_4)_6CO_3\square$, $Ba_{10}(PO_4)_6CO_3\square$ and $Sr_{10}(AsO_4)_6CO_3\square$], the incorporation of CO_3^{2-} ions into the *c*-axis anion channels has been shown to be of the type:

$$CO_3^{2-} + \square = 2\, F^- \qquad\qquad (2a)$$

(Mohseni-Koutchesfehani 1961; Bonel 1972; Baran et al. 1983; Hitmi et al. 1986). Polarized IR studies (Elliott 1964) suggested that the planar CO_3^{2-} ions in the anion channels are oriented approximately parallel to the *c*-axis to minimize the steric strain related to the incorporation of this large ion (Gruner and McConnell 1937). This configuration has recently been confirmed by single-crystal X-ray structure refinement of a flux-grown, A-type carbonate apatite (Suetsugu et al. 2000).

Trombe and Montel (1978) reported the presence of the peroxide O_2^{2-} ions in OHAp and A-type carbonate-bearing apatites that have been heated in dry oxygen. They proposed a reaction between OHAp and O_2 at 900°C:

$$Ca_{10}(PO_4)_6(OH)_{2-2x}(O^{2-})_x\square_x + 1/2\, yO_2 \rightarrow Ca_{10}(PO_4)_6(OH)_{2-2x}(O^{2-})_{x-y}(O_2^{2-})_y\square_x$$

where some of the O^{2-} ions in the OHAp anion channels are oxidized to the O_2^{2-} ions without any disruption of other structural constituents. Similarly, Trombe and Montel (1981) reported the presence of the cyanamide ions, NCN^{2-}, in the *c*-axis anion channels, as indicated by the formation of $Ca_{10}(PO_4)_6(NCN)\square$ from heating of A-type carbonate apatite in an atmosphere of NH_3 at 600 to 900°C. Dowker and Elliott (1983) suggested that the NCN^{2-} ions may be located at a position similar to that of NCO^- ions. Dugas et al. (1978) suggested that the nonlinear NO_2^{2-} ions are also present in the anion channels and oriented with the O-O direction parallel to the *c*-axis.

Neutral molecules and organic molecules. Neutral molecules, including H_2O, O_2, and CO_2, have been proposed to occur in the apatite *c*-axis anion channels (e.g., Joris and Amberg 1971; Rey et al. 1978a; Tochon-Danguy et al. 1978; Ivanova et al. 2001). Similarly, Tochon-Danguy et al. (1978) suggested that Ar is most likely trapped in the *c*-axis anion channels in enamel and bone powder samples, after they were subjected to low-temperature ashing in the presence of excited Ar gas molecules. Organic molecules such as glycine (Rey et al. 1978b), acetate (Bacquet et al. 1981a), and amino-2-ethylphosphate (Bonel et al. 1988) also have been reported to occur in the *c*-axis anion channels of OHAp precipitated from aqueous solutions containing the respective organic molecules.

Substitutions for calcium (M cations)

A large number of divalent cations (Sr^{2+}, Pb^{2+}, Ba^{2+}, Mn^{2+}, etc.) have been reported to substitute for Ca in the apatite-group minerals. Similarly, many monovalent (e.g., Na^+),

trivalent (REE^{3+}), tetravalent (Th^{4+} and U^{4+}), and hexavalent cations (U^{6+}; Rakovan et al. 2002) commonly occur in significant quantities in apatites and may substitute for Ca. In addition, Ca-deficiency (i.e., □) has been reported to occur in both natural and synthetic apatites, especially in biogenic apatites (e.g., Elliott 1994; Wilson et al. 1999; Suetsugu et al. 2000; Ivanova et al. 2001). There are two Ca sites in the apatite structure: nine-coordinated Ca1 and seven-coordinated Ca2 (Hughes et al. 1989). Therefore, possible cation ordering between these Ca positions is not only of intrinsic interest in structural studies of the apatite-group minerals but has important implications for substitution mechanisms.

Proposed substitutions at the Ca sites include:

$$M^{2+} = Ca^{2+} \qquad\qquad (7)$$
$$\square + 2\,\square = Ca^{2+} + 2\,F^- \qquad\qquad (4)$$
$$\square + 2\,ZO_4^{2-} = Ca^{2+} + 2\,PO_4^{3-} \qquad\qquad (8)$$
$$M^+ + \square = Ca^{2+} + F^- \qquad\qquad (3)$$
$$2\,M^+ = Ca^{2+} + \square \qquad\qquad (9)$$
$$M^+ + M^{3+} = 2\,Ca^{2+} \qquad\qquad (10)$$
$$M^+ + ZO_4^{2-} = Ca^{2+} + PO_4^{3-} \qquad\qquad (11)$$
$$M^{3+} + X^{2-} = Ca^{2+} + F^- \qquad\qquad (6)$$
$$M^{3+} + ZO_4^{4-} = Ca^{2+} + PO_4^{3-} \qquad\qquad (12)$$
$$2\,M^{3+} + \square = 3Ca^{2+} \qquad\qquad (13)$$
$$2\,M^{3+} + ZO_4^{5-} = 2\,Ca^{2+} + PO_4^{3-} \qquad\qquad (14)$$
$$M^{4+} + \square = 2\,Ca^{2+} \qquad\qquad (15)$$
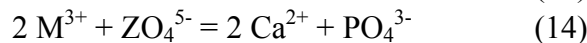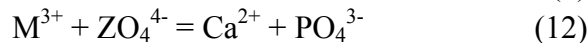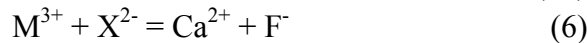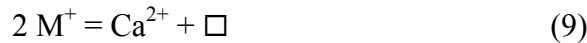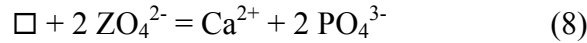
Divalent cations. Strontium is one of the most common M cation substituents in apatites and forms extensive solid solution series with Ca in natural apatites (Efimov et al. 1962; Pushcharovskii et al. 1987; Hughes et al. 1991a; Rakovan and Hughes 2000; Chakhmouradian et al. 2002). In addition, there are several Sr minerals of the apatite group: belovite-(La), belovite-(Ce), deloneite-(Ce), and strontium-apatite (Table 1). Also, complete solid solution series between Ca and Sr end-members have been established experimentally for FAp, OHAp, and ClAp (Khudolozhkin et al. 1972; 1973a; Heijligers et al. 1979; Sudarsanan and Young 1980; Khattech and Jemal 1997). Despite early contradictory results on the Ca site occupancy of Sr (e.g., Khudolozhkin et al. 1972; 1973a; Heijligers et al. 1979), it is now well established that Sr almost exclusively occupies the Ca2 site (or equivalent sites) in apatite structures (Sudarsanan and Young 1974, 1980; Hughes et al. 1991a; Bigi et al. 1998; Rakovan and Hughes 2000). Sudarsanan and Young (1980) also found that the site preference of Sr for Ca2 decreases with increase in the content of Sr and that the Cl position shifts from (0,0,0.44) in pure ClAp (Mackie et al. 1972; Hughes et al. 1989) to (0,0,1/2) in SrClAp at or above 48% of the replacement of Ca by Sr. This new location of the Cl^- ions leads to the formation of the SrO_6Cl_2 polyhedron in $Sr_{10}(PO_4)_6Cl_2$ (Sudarsanan and Young 1980). Similarly, Rakovan and Hughes (2000) reported the presence of the SrO_6Cl_2 polyhedron in a Cl-bearing belovite-(Ce), on the basis of the location of Cl^- ions at (0,0,1/2).

Complete solid solutions between Pb and Ca end-members have been synthesized for OHAp and ClAp (Akhavan-Niaki 1961; Engel et al. 1975; Miyake et al. 1986), although Verbeeck et al. (1981) noted a miscibility gap in OHAp at 800°C. Single-crystal and powder XRD studies on Pb apatites synthesized at elevated temperatures revealed that the Pb^{2+} ions have a strong preference for Ca2 sites (Engel et al. 1975; Hata et al. 1980; Mathew et al. 1980; Verbeeck et al. 1981), as that in caracolite (Schneider 1967). Engel et al. (1975) attributed this strong preference to the ability of Pb^{2+} cations to form partial covalent bonds (e.g., Pb2-O2 = 2.238 Å in $Pb_8K_2(PO_4)_6\square_2$; Mathew et al. 1980). One notable exception to this general trend is the study of Miyake et al. (1986) who, on the

basis of Rietveld XRD refinements of Pb^{2+} ion-exchanged OHAp, ClAp, and FAp, suggested that Pb^{2+} ions have no preference for Ca1 or Ca2 sites.

A complete solid solution between Ba and Ca end-members has been confirmed for ClAp (Table 4), whereas large miscibility gaps are known to exist in FAp and OHAp (e.g., between 6 and 61 mol % $Ba_{10}(PO_4)_6F_2$ in FAp at 900-1100°C; Akhavan-Niaki 1961; Bigi et al. 1984). Similarly, natural Cl-poor apatites contain only small amounts of Ba (up to 12.54 wt % BaO; Edgar 1989). Khudolozhkin et al. (1973a) showed that Ba^{2+} ions have preference for Ca2 sites and that this preference increases with increase in the content of Ba. Also, this site preference is more marked in the Ca-Ba apatites than in the Sr-Ba apatites (Khudolozhkin et al. 1973a).

Table 4. Solubility limits of some divalent cations in apatites $Ca_{10-n}M_n(PO_4)_6X_2$.

M	*X*	*n*	*References*
Sr	F	10	Akhavan-Niaki (1961), Khattech & Jamel (1997)
	OH	10	Heijligers et al. (1979)
	Cl	10	Akhavan-Niaki (1961)
Ba	F	0.6	Akhavan-Niaki (1961)
	Cl	10	Akhavan-Niaki (1961)
Pb	OH	10?	Engel et al. (1975), Verbeeck et al. (1981)
	Cl	10	Kreidler & Hummel (1970)
Cd	F	10	Akhavan-Niaki (1961) Kreidler & Hummel (1970)
	OH	10	Bigi et al. (1986)
	Cl	10	Klement & Haselbeck (1965)
Mg	F	0.9	Kreidler & Hummel (1970)
	OH	10?	Patel (1980); Chiranjeevirao et al. (1982)
	Cl	3.0	Klement & Haselbeck (1965)
Fe	F	1.5	Khudolozhkin et al. (1974)
Mn	F	1.37	Ercit et al. (1994)
	Cl	10	Klement & Haselbeck (1965)
Co	F	1.5	Grisafe & Hummel (1970)
	Cl	2.5	Grisafe & Hummel (1970)
Ni	F	0.75	Kreidler & Hummel (1970)
	F	1.0	Brasseur & Dallemagne (1949)
	Cl	3.0	Klement & Haselbeck (1965)
Cu	Cl	4.0	Klement & Haselbeck (1965)
Zn	F	1.0	Brasseur & Dallemagne (1949)
Sn	F	5.0	Klement & Haselbeck (1965)
	Cl	8.0	Klement & Haselbeck (1965)

Note that the reported complete solid solutions between Pb and Ca in OHAp and between Mg and Ca in OHAp are questionable (see text for discussion).

The substitution of Mn in apatites has been extensively investigated because Mn-doped FAp is used in the fluorescent-light industry, and Mn is ubiquitous in natural apatites. The maximum content of 1.37 Mn atoms per formula unit (apfu) in natural FAp (Ercit et al. 1994; see also Hughes et al. 1991a) exceeds the early proposed limit of 1 Mn

apfu (Suitch et al. 1985). A more extensive solid solution between Ca and Mn may exist in ClAp, as indicated by the synthesis of pure manganese ClAp (Table 4; Klement and Haselbeck 1965). There is a general consensus that Mn^{2+} ions have a strong preference for the Ca1 sites (Ryan et al. 1972; Warren and Mazelsky 1974; Suitch et al. 1985; Hughes et al. 1991a; Pan et al. 2002a). Manganese in the most Mn-rich FAp, however, shows only a slight preference for Ca1 (64%) (Ercit et al. 1994). This disordering in the Mn-rich FAp is consistent with the EPR results of Warren (1970), who showed that the site preference of Mn for Ca1 decreases with increase in the Mn content (see also Warren and Mazelsky 1974). Ryan et al. (1972) suggested that the site preference of Mn for Ca1 is greater in CaFAp than that in SrFAp. Ohkubo (1968) reported that the EPR signal of Mn^{2+} at Ca1 (i.e., center Mn_I) decreases with increase in the Cl content in binary Cl-FAp. Warren and Mazelsky (1974) also showed that the signal from Mn^{2+} at the Ca2 site (Mn_{II}) in CaF_2-deficient FAp is very weak and is replaced by a different signal from Mn in a modified Ca2 site (i.e., Mn_{IIm}). Warren and Mazelsky (1974) noted that the signal intensity from Mn_{II} increases with increase in the Mn/Ca value, whereas the Mn_{IIm} signal intensity decreases. Warren and Mazelsky (1974) associated the Mn_{IIm} center with the $(\square O\square)^+$ defect (Warren 1972; see above). Suitch et al. (1985) suggested that incorporation of Mn into FAp results in a reduction of symmetry to $P6_3$ or $P3$. This suggestion, however, was not supported by studies of natural Mn-rich FAp (Hughes et al. 1991a; Ercit et al. 1994).

Iron occurs only as a minor to trace element and rarely exceeds 1 wt % as FeO in natural apatites (up to 2.2 wt % FeO; Fransolet and Schreyer 1981). Khudolozhkin et al. (1974) reported that the solubility limit of Fe in FAp is ~15 mol % replacement of Ca^{2+} by Fe^{2+} (Table 4). Their Mössbauer spectroscopic study suggested that Fe^{2+} is randomly distributed between the Ca1 and Ca2 sites in Fe-poor FAp (<1 mol %), but has a strong preference for Ca1 at high concentrations towards the solubility limit of Fe^{2+} in FAp. These results, however, are opposite to that of Hughes et al. (1993) who, on the basis of a single-crystal X-ray structural refinement of a natural, Fe-bearing monoclinic FAp, showed that Fe^{2+} preferentially occupies Ca2-equivalent sites.

Although Mg appears to have a limited solubility in FAp (Table 4), a complete replacement of Ca by Mg has been reported for OHAp (Patel 1980; Chiranjeevirao et al. 1982). However, an attempt by Terpstra and Driessens (1986) to confirm the results of Chiranjeevirao et al. (1982) was unsuccessful. Neuman and Mulryan (1971) showed that nearly 90% of the Mg in OHAp precipitated from Mg^{2+}-bearing solutions is readily exchangeable and, hence, is most likely located at surface positions. In synthetic $Mg_2REE_8(SiO_4)_6O_2$, Mg^{2+} appears to preferentially occupy Ca1 sites and may alternate with the REE^{3+} ions (Ito 1968).

Other divalent cations, which substitute for Ca^{2+} in apatites, include Ni^{2+}, Co^{2+}, Cu^{2+}, Zn^{2+}, Sn^{2+}, Cd^{2+} (Table 4), and Eu^{2+} (Table 3). The solubility limits for Co^{2+} in FAp and ClAp are 15 and 25 mol %, respectively, but are less than 10 mol % in the Sr analogs (Grisafe and Hummel 1970). Single-crystal X-ray refinements of Co-bearing ClAp showed that the Co^{2+} ions are located exclusively at the Ca2 sites, with the Cl^- ions shifted along the c-axis toward the Co^{2+} ion to maintain a reasonable Co-Cl bond distance (Anderson and Kostiner 1987). A complete replacement of Ca^{2+} by Cd^{2+} has been demonstrated by the synthesis of various Cd apatites (Sudarsanan et al. 1977; Wilson et al. 1977; Hata et al. 1978; Bigi et al. 1986; Christy et al. 2001). A cadmium K-edge EXAFS study by Sery et al. (1996) suggested that Cd occupies both Ca sites with a slight preference for Ca2. The presence of Eu^{2+} in apatites has been well established for synthetic materials (Mayer et al. 1975) and has been confirmed by a synchrotron wavelength dispersive XANES study on natural FAp (Rakovan et al. 2001). Rakovan et al. (2001) also suggested that the presence of both Eu^{2+} and Eu^{3+} is most likely responsible for the abnormal partitioning behavior of

Eu, relative to other REEs, between the <001> and <011> sectors in the Llallagua FAp crystals investigated by Rakovan and Reeder (1994, 1996).

Monovalent cations. Sodium is a common minor constituent in natural calcium phosphate apatites (e.g., Roeder et al. 1987; Rønsbo 1989; Comodi et al. 1999) and becomes a major component in belovite-(La), belovite-(Ce), deloneite-(Ce), cesanite, caracolite, and many synthetic apatites (Table 3). Potassium, Li, and Rb are only trace constituents in natural apatites, but attain significant concentrations in some synthetic apatites (e.g., Schwarz 1967a; Simpson 1968; Mathew et al. 1980). These monovalent cations in apatites have been shown to have strong preference for the Ca1 sites (Calvo et al. 1975; Mathew et al. 1979; Fleet and Pan 1997a; Takahashi et al. 1998; Rakovan and Hughes 2000) and commonly involve REE^{3+} ions (see below) or other coupled substitutions (e.g., CO_3^{2-} or SO_4^{2-} for PO_4^{3-}; see below) to preserve electrostatic neutrality.
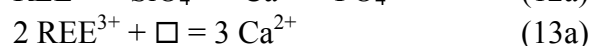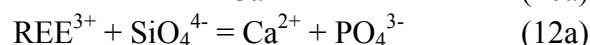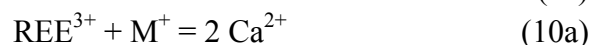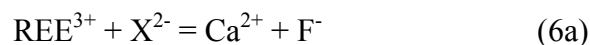
Other monovalent ions that have been proposed to substitute for Ca^{2+} in apatites include NH_4^+ and H_3O^+ (McConnell 1952; Simpson 1968; Doi et al. 1982; Vignoles et al. 1987). For example, McConnell (1952) and Simpson (1968) postulated the presence of H_3O^+ as replacement for Ca^{2+} in Ca-deficient OHAp; however, this was questioned by Elliott (1969), because this ion is generally restricted to the structure of strong acids. The NH_4^+ ion has been shown to occur (at up to 0.12 wt % N) in carbonate apatites precipitated from NH_4^+-bearing solutions (Doi et al. 1982; Vignoles et al. 1987). Doi et al. (1982) suggested that NH_4^+ may substitute for Ca^{2+} via:

$$2\,NH_4^+ = Ca^{2+} + \square \qquad\qquad (9a)$$

Ivanova et al. (2001) interpreted a slight decrease of atomic scattering at the Ca2 site in a synthetic, NH_4^+-bearing apatite to a preferential incorporation of NH_4^+ ions into this site.

Trivalent cations. Apatite-group minerals have long been known as important hosts for REEs and Y in igneous, metamorphic, and sedimentary rocks (e.g., Watson et al. 1985; Roeder et al. 1987; Rønsbo 1989; Hughes et al. 1991b; Fleet and Pan 1995a; Gaft et al. 1997' Pan and Breaks 1997) and in the biomass as well (e.g., Wright et al. 1984; Grandjean-Lécuyer et al. 1993; Holmden et al. 1996, 1998). The ability of apatites to accommodate significant amounts of REEs and Y is also demonstrated by the formation of many natural and synthetic REE apatites (Tables 1, 2, and 3; Cockbain and Smith 1967; Ito 1968; Felsche 1972; Steinbruegge et al. 1972; Mayer et al. 1974; Azimov et al. 1981; Mayer and Cohen 1983). Although early studies on REE site preference yielded contradictory results (e.g., Ca1, Urusov and Khudolozhkin, 1974; Ca2, Borisov and Klevtsova 1963), recent X-ray structure refinements of natural and synthetic apatites have all shown that REEs in FAp, OHAp, and OAp generally prefer the Ca2 site and that the site-occupancy ratios (REE-Ca2/REE-Ca1) decrease monotonically with increase in atomic number through the 4f transition series (Hughes et al. 1991b, 1992; Fleet and Pan 1994, 1995a, 1997a; Takahashi et al. 1998; Fleet et al. 2000a; Serret et al 2000). However, Fleet et al. (2000b) showed that REEs in ClAp preferentially occupy the Ca1 equivalent sites, with the exception of Nd, which has a marginal preference for the Ca2 equivalent sites [(Nd-Ca2/Nd-Ca1) = 1.11].

Four main types of charge-compensating mechanisms have been proposed for the substitution of Ca^{2+} by REE^{3+} (and Y^{3+}) in apatites (Ito 1968; Felsche 1972; Roeder et al. 1987; Rønsbo 1989; Fleet and Pan 1995a; Comodi et al. 1999; Cherniak 2000; Serret et al. 2000; Chen et al. 2002a,b):

$$REE^{3+} + X^{2-} = Ca^{2+} + F^- \qquad\qquad (6a)$$
$$REE^{3+} + M^+ = 2\,Ca^{2+} \qquad\qquad (10a)$$
$$REE^{3+} + SiO_4^{4-} = Ca^{2+} + PO_4^{3-} \qquad\qquad (12a)$$
$$2\,REE^{3+} + \square = 3\,Ca^{2+} \qquad\qquad (13a)$$

Substitution (6a), involving concomitant replacement of O^{2-} or S^{2-} ions for F^- ions in the c-axis anion channels, has been demonstrated by the synthesis of $Ca_8REE_2(PO_4)_6O_2$ (e.g., Ito 1968; Schroeder and Mathew 1978; Piriou et al. 1987; Serret et al. 2000) and $Ca_{10-x}Eu_x(PO_4)_6S_{1+x/2}\square_{1-x/2}$ (Suitch et al. 1986; Taïtaï and Lacout 1989). Single-crystal EPR studies of synthetic FAp containing 1.2 wt % Gd_2O_3 (Chen et al. 2002a) and 97 ppm [157]Gd (Chen et al. 2002c) revealed the presence of a Gd^{3+} center 'a', corresponding to occupancy of Gd^{3+} ions at Ca2 sites, and that the center 'a' has a rhombic (i.e., triclinic) local symmetry, different from a uniaxial symmetry expected for the ideal Ca2 site in pure FAp. This distortion was interpreted to be related to a replacement (and minor displacement away from z = 1/4 or 3/4; cf. Fleet al. 2000a) of O^{2-} for F^- in the c-axis anion channel (Chen et al. 2002a).
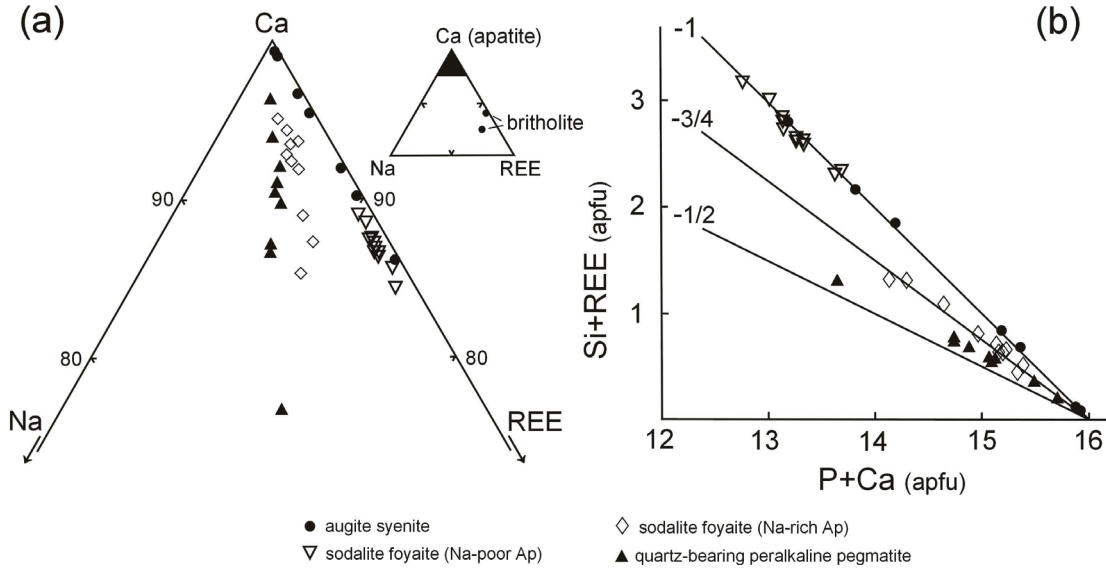
Figure 2. Substitution of REEs into apatite from the Ilímaussaq intrusion, South Greenlend: (a) molar proportion of Ca, REEs and Na; (b) (Si+REE) apfu *versus* (P+Ca) atoms per formula unit (apfu). Line of slope -1 represents the coupled substitution: $REE^{3+} + SiO_4^{4-} = Ca^{2+} + PO_4^{3-}$. Note that apatite compositions from Na-rich sodalite foyaite and quartz-bearing peralkaline pegmatite reflect progressively increasing importance of the substitution: $REE^{3+} + Na^+ = 2Ca^{2+}$ (after Rønsbo 1989).

Substitution (10a) is well established on the basis of compositional data from natural apatites (e.g., Roeder et al. 1987; Rønsbo 1989; Peng et al. 1997; Comodi et al. 1999; Fig. 2), and is largely responsible for accommodating REEs into belovites (e.g., Pekov et al. 1996; Rakovan and Hughes 2000). Although the end-member composition $Na_5REE_5(PO_4)_6F_2$ for this substitution is known to be unstable, intermediate compositions such as $Na_4REE_4Ca_2(PO_4)_6F_2$ have been synthesized (Mayer et al. 1974). Other monovalent cations that have been shown to participate in this type of coupled substitution for the incorporation of REE^{3+} into synthetic apatites include Li^+ (Ito 1968; Felsche 1972) and Ag^+ (Mayer and Swissa 1985).

Substitution (12a) is also well documented in natural REE-bearing apatites (Fig. 2; Roeder et al. 1987; Rønsbo 1989; Comodi et al. 1999), and is supported by a complete solid solution between OHAp and britholite-(Y) (Ito 1968; Khudolozhkin et al. 1973b). This substitution leads to the end-member $Ca_4REE_6(SiO_4)_6F_2$, which has been synthesized for compositions involving La, Ce, Nd, and Y (Ito 1968; Mayer et al. 1974).

Substitution (13a), involving a vacancy at Ca sites, is partly responsible for the accommodation of REEs in synthetic $\square CaREE_8(SiO_4)_6F_2$ and $\square_2REE_8(SiO_4)_6\square_2$ (Grisafe and Hummel 1970). Chen et al. (2002b), on the basis of an EPR study on flux-grown FAp crystals containing 57 ppm Gd, detected a Gd^{3+} center 'b' corresponding to occupancy of

Gd^{3+} ions at the Ca1 sites. Chen et al. (2002b) showed that the Gd^{3+} center 'b' has a highly triclinic local symmetry, different from the uniaxial symmetry of the ideal Ca1 site in pure FAp. Chen et al. (2002b) suggested that the triclinic symmetry of this Gd^{3+} center is related to the presence of a vacancy at the next-nearest-neighbor Ca2 site, resulting in a Gd^{3+} -- □ -- Gd^{3+} arrangement, with the cations well separated.

Another extensively investigated trivalent cation in apatites is Sb^{3+}, because Sb-doped FAp acts as an activator in fluorescent-light tubes (e.g., Davis et al. 1971; Soules et al. 1971; Mishra et al. 1987; DeBoer et al. 1991; Moran et al. 1992). Rietveld XRD refinements of a FAp powder sample with 2.2 wt % Sb suggested that Sb^{3+} is ordered at the Ca2 site (DeBoer et al. 1991), consistent with the site occupancy deduced from excitation and emission spectra of Sb-doped ClAp and FAp (Davis et al. 1971; Soules et al. 1971). However, the same study on a different sample containing 3.1 wt % Sb did not find any evidence for substitution at the Ca2 site but suggested, on the basis of electron density maps, that the Sb^{3+} ions occupy the (1/3,2/3,1/4) and (2/3,1/3,1/4) sites (DeBoer et al. 1991). Also, the Ca2 site assignment for Sb^{3+} ions is not consistent with results from ^{121}Sb Mössbauer (Mishra et al. 1987) or ^{19}F and ^{31}P MAS NMR studies (Moran et al. 1992; see below).

Other trivalent cations that have been shown to substitute for Ca in synthetic oxyapatites include Bi^{3+} and Cr^{3+} (Table 2). The composition of $Bi_2Ca_8(PO_4)_6O_2$ (Buvaneswari and Varadaraju 2000) suggests a coupled substitution of the type:

$$Bi^{3+} + O^{2-} = Ca^{2+} + F^- \qquad (6b)$$

Huang and Sleight (1993) showed that Bi^{3+} ions in $Bi_2Ca_8(VO_4)_6O_2$ preferentially occupy Ca1 sites (see also Mayer and Semadja 1983), whereas Cr^{3+} ions in $Cr_2Sm_8(SiO_4)_4(SiO_3N)_2O_2$ were found to reside exclusively in Ca2 sites (Maunaye et al. 1976). Mayer and Semadja (1983) also noted that Bi tends to favor apatites with vacant anion channels.

Tetravalent cations. Elevated amounts of Th have been reported for natural apatites, particularly in the REE-rich varieties [e.g., up to 15.9 wt % ThO_2 in britholite-(Ce)] from alkaline and peralkaline igneous rocks (Hughson and Sen Gupta 1964; Arden and Halden 1999; Della-Ventura et al. 1999; Oberti et al. 2001). Uranium is also a common, minor to trace element (up to 3.4 wt % UO_2) in natural apatites (Clarke and Altschuler 1958; Arden and Halden 1999; Della-Ventura et al. 1999; Oberti et al. 2001), although the U contents in apatites from some early studies may be overestimated owing to the common occurrences of U-rich inclusions (Baumer et al. 1983). Compositional data (Hughson and Sen Gupta 1964; Baumer et al. 1983) have shown that Th^{4+} ions substitute for Ca^{2+} via:
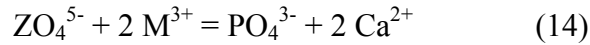
$$Th^{4+} + \square = 2\ Ca^{2+} \qquad (15a)$$

Similarly, Clarke and Altschuler (1958) suggested that U in apatites is mainly tetravalent and that U^{4+} ions occupy the Ca sites via a similar substitution (Baumer et al. 1983):

$$U^{4+} + \square = 2Ca^{2+} \qquad (15b)$$

Substitutions for phosphate (ZO₄ group)

The PO_4^{3-} group in the apatite-group minerals is commonly replaced by a variety of other tetrahedral anion groups (e.g., AsO_4^{3-}, VO_4^{3-}, MnO_4^{3-}, CrO_4^{3-}, SO_4^{2-}, SeO_4^{2-}, CrO_4^{2-}, BeF_4^{2-}, SiO_4^{4-}, GeO_4^{4-}, SbO_3F^{4-}, SiO_3N^{5-}, and BO_4^{5-}). Another tetrahedral anion group proposed by McConnell (1973) to substitute for PO_4^{3-} is $(OH)_4^{4-}$, by analogy to that in "hydrogarnets" (Nobes et al. 2000; Armbruster et al. 2001 and references therein). But to our knowledge, no structural evidence for the $(OH)_4^{4-}$ group has been found in the apatite-group minerals or their synthetic analogs. Other polyhedral groups that have been shown to substitute for PO_4^{3-} in the apatite-group minerals include CO_3^{2-}, BO_3^{3-}, and ReO_5^{3-}. Propos-ed mechanisms for the replacement of the PO_4^{3-} group in the apatite-group minerals include:

$$ZO_4^{3-} = PO_4^{3-} \qquad\qquad (16)$$

$$2\, ZO_4^{2-} + \square = 2\, PO_4^{3-} + Ca^{2+} \qquad\quad (8)$$

$$ZO_4^{2-} + M^+ = PO_4^{3-} + Ca^{2+} \qquad (11)$$

$$ZO_4^{2-} + ZO_4^{4-} = 2\, PO_4^{3-} \qquad\quad (17)$$

$$ZO_4^{4-} + \square = PO_4^{3-} + F^- \qquad\qquad (5)$$

$$ZO_4^{4-} + M^{3+} = PO_4^{3-} + Ca^{2+} \qquad (12)$$

$$ZO_4^{5-} + 2\, M^{3+} = PO_4^{3-} + 2\, Ca^{2+} \qquad (14)$$
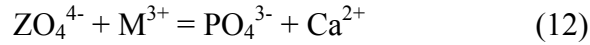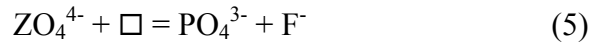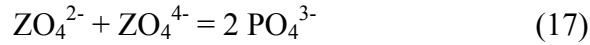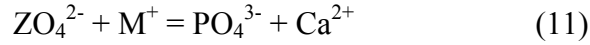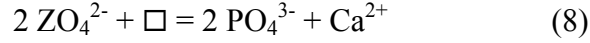
Trivalent anion groups. Extensive substitution of the PO_4^{3-} group by the tetrahedrally coordinated and isovalent AsO_4^{3-} ion has been well established by the existence of a complete solid solution between pyromorphite and mimetite (Kautz and Gubser 1969; Förtsch and Freiburg 1970) and by data from As-bearing FAp (Persiel et al. 2000 and references therein). One notable exception is the study of Bothe and Brown (1999), who observed no solid solution between $Ca_{10}(PO_4)_6(OH)_2$ and $Ca_{10}(AsO_4)_6(OH)_2$ at ambient temperatures. Hughes and Drexler (1991) showed that replacement of PO_4^{3-} by AsO_4^{3-} in fermorite causes little disruption in the atomic arrangement of this mineral and that there is no evidence of ordering accompanying the substitution:

$$AsO_4^{3-} = PO_4^{3-} \qquad\qquad (16a)$$

Other tetrahedrally coordinated and trivalent ions that have been shown to substitute for the PO_4^{3-} group include VO_4^{3-}, MnO_4^{3-}, and CrO_4^{3-} (Banks and Jaunarajs 1965; Kingsley et al. 1965; Sudarsanan et al. 1977; Huang and Sleight 1993). Vanadinite and synthetic vanadate apatites indicate the substitution (Sudarsanan et al. 1977; Dai and Hughes 1989; Huang and Sleight 1993):

$$VO_4^{3-} = PO_4^{3-} \qquad\qquad (16b)$$
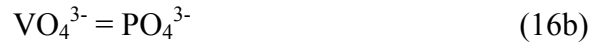
and a complete solid solution series between $Ca_{10}(PO_4)_6F_2$ and $Ca_{10}(VO_4)_6F_2$ has been confirmed by Kreidler and Hummel (1970). Kingsley et al. (1965) showed the presence of MnO_4^{3-} ions as replacement for PO_4^{3-} ions in $MnCl_2$ flux-grown ClAp. Similarly, replacement of PO_4^{3-} ions by CrO_4^{3-} ions in synthetic apatites was reported by Banks and Jaunarajs (1965) and Banks et al. (1971).

Other trivalent ions that have been suggested to substitute for PO_4^{3-} include SbO_3^{3-}, BO_3^{3-}, and ReO_5^{3-} (Calvo et al. 1975; Ito et al. 1988; Mishra et al. 1987; Moran et al. 1992; Schriewer and Jeitschko 1993). For example, an [121]Sb Mössbauer study by Mishra et al. (1987) suggested that Sb in Sb-doped FAp occurs as the SbO_3^{3-} ion, which may be coordinated with F^- as the fourth ligand to form the SbO_3F^{4-} group. Also, the presence of SbO_3^{3-} ions in Sb-doped FAp is supported by results from ^{19}F and ^{31}P MAS NMR studies (Moran et al. 1992). Ito et al. (1988) showed, on the basis of isotopic frequency shifts (IR), the presence of BO_3^{3-} as replacement for PO_4^{3-} in [11]B- and [10]B-doped apatites. Schriewer and Jeitschko (1993) emphasized that the apex oxygen atoms of the pyramidal ReO_5^{3-} groups in $Ba_{10}(ReO_5)_6Cl_2$ all point approximately down the *c*-axis, resulting in the loss of the horizontal mirror plane (see also Besse et al. 1979).

Divalent anion groups. Extensive substitution between SO_4^{2-} and PO_4^{3-} has been demonstrated by compositional data from natural apatites (McConnell 1937; Schneider 1967; Rouse and Dunn 1982; Hughes and Drexler 1991; Liu and Comodi 1993; Peng et al. 1997; Comodi et al. 1999) and is supported by the synthesis of various sulfate apatites (e.g., Schwarz 1967a,b; Kreidler and Hummel 1970; Khorari et al. 1994). Common correlations between the Si and S contents in natural apatites (Rouse and Dunn 1982; Baumer et al. 1990; Liu and Comodi 1993; Peng et al. 1997; Comodi et al. 1999; Steele et al. 2000) indicate a charge-compensating mechanism of the type:
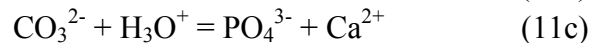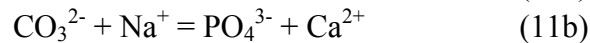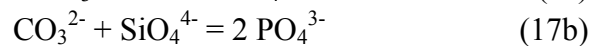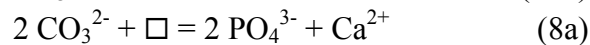
$$SO_4^{2-} + SiO_4^{4-} = 2\ PO_4^{3-} \qquad (17a)$$
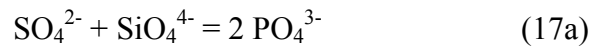
For example, Rouse and Dunn (1982) reported that SO_4^{2-} and SiO_4^{4-} in ellestadites occur in consistently equal proportions, suggesting a possible ordering of Si and S in the ellestadite structure. Sudarsanan (1980) showed that the equivalent tetrahedral sites in the $P6_3/m$ structure split into 3 non-equivalent T1, T2 and T3 sites in monoclinic hydroxylellestadite and that some degree of Si-S ordering does appear to occur. This observation has since been confirmed by Hughes and Drexler (1991), who showed that the Si^{4+} and S^{6+} ions in monoclinic hydroxylellestadite preferentially occupy the T1 and T2 sites, respectively, and that the T3 site is occupied by both ions in approximately equal proportions. Khorari et al. (1994), however, did not find any evidence for Si-S ordering in synthetic FAp. Compositional data from natural and synthetic FAp (Liu and Comodi 1993; Peng et al. 1997) also indicate a substitution of the type:

$$SO_4^{2-} + Na^+ = PO_4^{3-} + Ca^{2+} \qquad (11a)$$
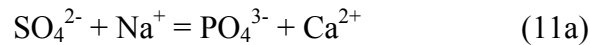
This substitution, however, appears to be less important than Substitution (17a) (Peng et al. 1997).

The common occurrence of B-type carbonate-bearing apatite involving replacement of the PO_4^{3-} group by CO_3^{2-} is now well established (McConnell 1973; Elliott 1994; Ivanova et al. 2001). Polarized IR studies suggested that the orientation of the CO_3^{2-} ion lies in the position of the sloping face of the replaced PO_4^{3-} tetrahedron (Elliott 1964). A Ca K-edge EXAFS study of carbonate-bearing OHAp showed that the coordination of the Ca^{2+} ions by the nearest-neighbor O atoms is not notably affected by the replacement of CO_3^{2-} for PO_4^{3-}, but marked changes in the transformation occur beyond 3 Å (Harries et al. 1987). These data led Harries et al. (1987) to suggest that the O atoms of the planar CO_3^{2-} ion occupy three of the four vacant O sites left by a PO_4^{3-} ion, and that the fourth O site is directed away from the CO_3^{2-} ion. A Rietveld XRD refinement of a synthetic, B-type carbonate-bearing OHAp by Ivanova et al. (2001) showed that the CO_3^{2-} ions randomly occupy the two vertical faces of the PO_4 tetrahedron (i.e., the faces with a common edge parallel to the c-axis).

Six charge-compensating mechanisms have been proposed for the incorporation of CO_3^{2-} ions into the PO_4^{3-} sites:

$$CO_3OH^{3-} = PO_4^{3-} \qquad (16c)$$
$$CO_3F^{3-} = PO_4^{3-} \qquad (16d)$$
$$2\ CO_3^{2-} + \square = 2\ PO_4^{3-} + Ca^{2+} \qquad (8a)$$
$$CO_3^{2-} + SiO_4^{4-} = 2\ PO_4^{3-} \qquad (17b)$$
$$CO_3^{2-} + Na^+ = PO_4^{3-} + Ca^{2+} \qquad (11b)$$
$$CO_3^{2-} + H_3O^+ = PO_4^{3-} + Ca^{2+} \qquad (11c)$$

The two substitutions involving CO_3OH^{3-} and CO_3F^{3-} were proposed mainly on the basis of compositional data from natural and synthetic carbonate-bearing apatites (e.g., $F^- + OH^- >$ 2 apfu; Borneman-Starynkevich 1938; Borneman-Starynkevich and Belov 1953; Trueman 1966; Labarthe et al. 1971; Vignoles and Bonel 1978; Sommerauer and Katz-Lehnert 1985; Binder and Troll 1989). These two substitutions are appealing in that the CO_3F^{3-} and CO_3OH^{3-} groups are tetrahedrally coordinated and are isovalent with the PO_4^{3-} group for which they substitute. However, evidence for the presence of CO_3F^{3-} and CO_3OH^{3-} groups from IR and EPR studies (e.g., Labarthe et al. 1971; Vignoles and Bonel 1978; Bacquet et al. 1980; 1981b) is ambiguous (Okazaki 1983; Elliott 1994; Regnier et al. 1994). Also, Okazaki (1983) and Jahnke (1984) found no clear positive correlation between the F^- and CO_3^{2-} contents in synthetic apatites. Indeed, no structural evidence for CO_3F^{3-} or CO_3OH^{3-} groups has been found in any of the ^1H, ^{19}F and ^{13}C NMR and EXAFS studies of natural and synthetic

carbonate-bearing apatites (e.g., Harries et al. 1987; Rey et al. 1989; Beshah et al. 1990; Regnier et al. 1994). Also, *ab-initio* quantum mechanical calculations suggested that CO_3F^{3-} is unstable in apatites and that the excess F^- ions in carbonate-bearing FAp most likely occupy an interstitial site (Regnier et al. 1994). Another variation of these two substitutions is replacement of $CO_3H_2O^{2-}$ for PO_4^{3-}, which also suffers from the lack of structural evidence for the existence of $CO_3H_2O^{2-}$ (Beshah et al. 1990).

X-ray structural data from synthetic carbonate-bearing apatites (Suetsugu et al. 2000) showed that the charge imbalance introduced when CO_3^{2-} replaces PO_4^{3-} is compensated primarily by Ca vacancies [i.e., Substitution (8a)]. However, uncertainties remain regarding the location of the associated vacancies (e.g., Ca2 site, Wilson et al. 1999; Ca1 site, Ivanova et al. 2001). The coupled substitution involving concomitant replacement of SiO_4^{4-} for PO_4^{3-} has been well established on the basis of compositional data from high-temperature FAp and OHAp in igneous rocks (e.g., Sommerauer and Katz-Lehnert 1985; Comodi et al. 1999). The coupled substitution involving parallel replacement of Na^+ for Ca^{2+} was also proposed on the basis of compositional data from natural carbonate-bearing apatites (McConnell 1952; Ames 1959), and has been confirmed by the synthesis of Na- and carbonate-bearing apatites (e.g., Bonel et al. 1973). On the other hand, the similar substitution involving concomitant replacement of H_3O^+ for Ca^{2+} (McConnell 1952; Simpson 1968) is less certain.

Two other divalent complex ions that have been shown to substitute for PO_4^{3-} in synthetic apatites are SeO_4^{2-} and CrO_4^{2-} (Schwarz 1967a,b). The compositions of $Pb_6K_4(PO_4)_4(SeO_4)_2\square_2$ and $Pb_6K_4(AsO_4)_4(SeO_4)_2\square_2$ (Schwarz 1967a) suggest a coupled substitution of the type:

$$SeO_4^{2-} + K^+ = PO_4^{3-} + Ca^{2+} \qquad (11d).$$
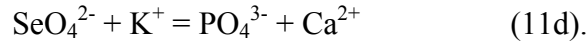
The compositions of $K_6Pb_4(CrO_4)_6F_2$ and $Sr_{10}(SiO_4)_3(CrO_4)_3F_2$ (Schwarz 1967b) suggest the charge-compensating mechanisms are respectively:

$$CrO_4^{2-} + K^+ = PO_4^{3-} + Ca^{2+} \qquad (11e)$$
$$CrO_4^{2-} + SiO_4^{4-} = 2\ PO_4^{3-} \qquad (17c)$$
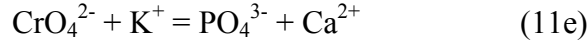
Tetravalent anion groups. A complete solid solution between OHAp and britholite-(Y), indicative of extensive substitution of PO_4^{3-} by SiO_4^{4-}, has been confirmed by data from both natural apatites and experimental synthesis (Ito 1968; Felsche 1972; Rouse and Dunn 1982; Roeder et al. 1987; Rønsbo 1989; Liu and Comodi 1993; Comodi et al. 1999). Two coupled substitutions of the type:

$$SiO_4^{4-} + REE^{3+} = PO_4^{3-} + Ca^{2+} \qquad (12a)$$
$$\text{and} \quad SiO_4^{4-} + (SO_4,CO_3)^{2-} = 2\ PO_4^{3-} \qquad (17a,b)$$
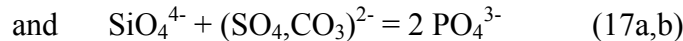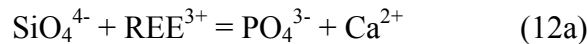
have been proposed for incorporating Si into apatites (Roeder et al. 1987; Rønsbo 1989; Liu and Comodi 1993; Comodi et al. 1999) and have been discussed above. Peng et al. (1997) showed that these two substitutions alone cannot account for the observed Si contents in their FAp synthesized from FMQ-buffered experiments and proposed an additional coupled substitution of the type:

$$SiO_4^{4-} + \square = PO_4^{3-} + F^- \qquad (5a)$$
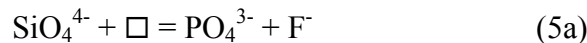
A replacement of GeO_4^{4-} ions for PO_4^{3-} ions is indicated by synthetic germanate apatites: $M_{10}(ZO_4)_3(GeO_4)_3F_2$ (M = Sr, Pb; Z = S, Cr) and $Sr_{10}(PO_4)_4(GeO_4)_2\square_2$ (Schwarz 1967b, 1968). These compositions suggest that the charge-compensating mechanisms for the incorporation of GeO_4^{4-} ions are of the type:

$$GeO_4^{4-} + (SO_4^{2-},CrO_4^{2-}) = 2\ PO_4^{3-} \qquad (17d,e)$$
$$GeO_4^{4-} + \square = PO_4^{3-} + F^- \qquad (5b)$$
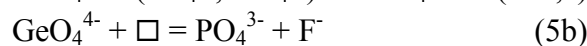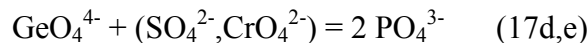
Frondel and Ito (1957) documented the substitution of GeO_4^{4-} for AsO_4^{3-} in natural mimetite.

Pentavalent anion groups. SiO_3N^{5-} ions have been suggested to occur in synthetic silicate oxyapatites (Gaudé et al. 1975; Maunaye et al. 1976; Guyader et al. 1978; Dupree et al. 1988; Harris et al. 1989), and are apparently incorporated via a coupled substitution of the type:

$$SiO_3N^{5-} + 2\ REE^{3+} = PO_4^{3-} + 2\ Ca^{2+} \quad\quad (14a)$$
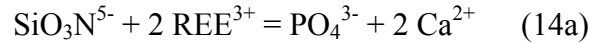
as indicated by the composition of $Sm_{10}(SiO_4)_4(SiO_3N)_2O_2$ (Gaudé et al. 1975).

It has been noted above that the synthetic rare-earth borosilicate oxyapatites of Ito (1968) suggest the presence of BO_4^{5-} ions (see also Mazza et al. 2000), which can be related to PO_4^{3-} in FAp via a coupled substitution of the type:

$$BO_4^{5-} + 2\ REE^{3+} = PO_4^{3-} + 2\ Ca^{2+} \quad\quad (14b)$$
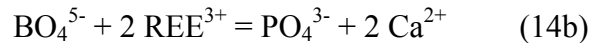
Ito (1968) also showed that there is a complete solid solution between $Ca_2Y_8(SiO_4)_6O_2$ and $Y_{10}(SiO_4)_4(BO_4)_2O_2$, where the exchange reaction is:

$$BO_4^{5-} + Y^{3+} = SiO_4^{4-} + Ca^{2+}.$$
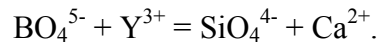
INTRINSIC AND EXTERNAL CONTROLS ON UPTAKE OF REEs IN APATITES

It is not possible to detail all of the factors that may influence the complex chemical variation in apatites (see also reviews by McConnell 1973; Roy et al. 1978; Elliott 1994), especially because data for many solid solutions are either incomplete or absent. Accordingly, we have selected the uptake of REEs in FAp, OHAp, and ClAp as examples to illustrate some of the important factors, both intrinsic (crystal-chemical) and external (P-T-X), that control the compositional variation in apatites.

Crystal-chemical controls

Data from natural apatites and laboratory experiments have shown that the uptake of REEs in natural apatites is highest in the range Nd-Gd, the peak in the uptake curve being near Nd for synthetic FAp (Fleet and Pan 1995b; 1997b), OHAp (Fleet et al. 2000a), and ClAp (Fleet et al. 2000b), while uptake is lowest for Lu (Figs. 3 and 4). Also, Watson and Green (1981) showed that the partition coefficient for Sm [D(Sm)] between FAp and melts of basanitic to granitic compositions is greater than those for La, Dy, and Lu. Similarly, Ayers and Watson (1993) reported that D(Gd) is greater than D(Ce) and D(Yb) for partitioning between FAp and aqueous fluids at 1.0 GPa and 1000°C. The overall consistency of this behavior for rocks, melts and fluids of widely different composition points to crystal-chemical controls on the uptake of REEs in apatites.

From systematic analysis of site occupancies and structural change in REE-substituted FAp, OHAp, and ClAp (Fleet and Pan 1994; 1995a; 1997a,b; Fleet et al. 2000a,b), Fleet et al. (2000b) noted that the crystal-chemical factors that control site preference and uptake of REEs in apatites are complex and include substitution mechanisms (Mackie and Young 1973), spatial accommodation, equalization of bond valence (Hughes et al. 1991b; Takahashi et al. 1998) and a possible crystal field contribution for Nd.

Substitution mechanisms. Fleet et al. (2000b) noted that different substitution mechanisms were responsible for the incorporation of REEs into synthetic apatites. For example, REEs in OHAp that crystallized from H_2O-bearing phosphate melts were charge-compensated by concomitant replacement of PO_4^{3-} by SiO_4^{4-}, i.e.,

$$REE^{3+} + SiO_4^{4-} = Ca^{2+} + PO_4^{3-} \quad\quad (12a)$$
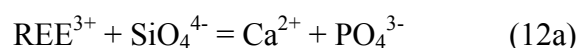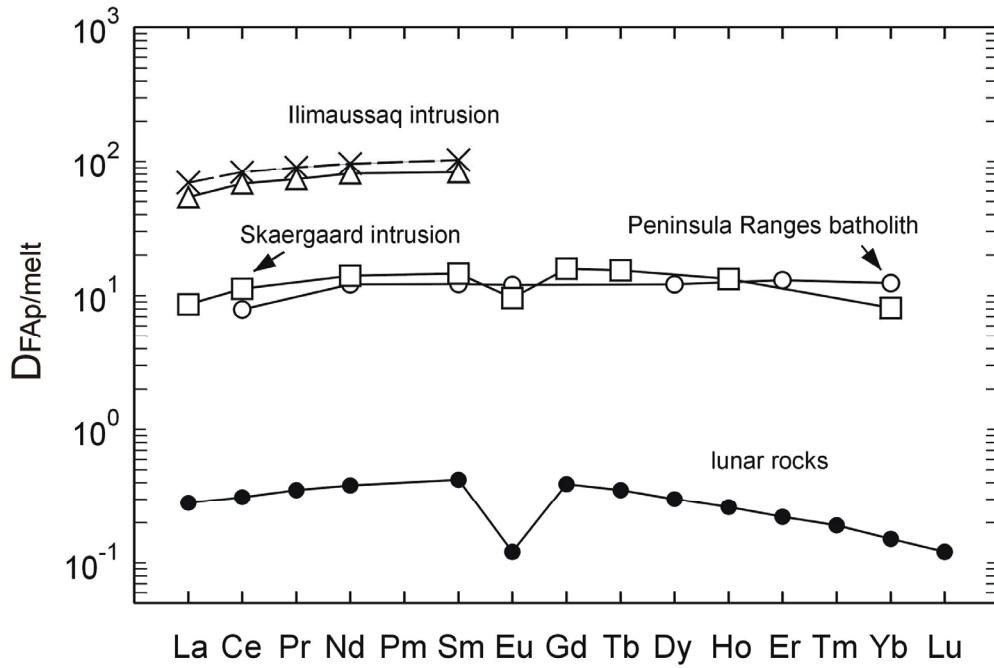
Figure 3. Melt-normalized REE patterns for fluorapatite (FAp) from lunar rocks (full circles; Jolliff et al. 1993), Skaergaard layered series, Greenland (upper zone, □; Paster et al. 1974), granodiorite from the eastern Peninsular Ranges batholith, southern California (apatite/whole rock data, ◖; Gromet and Silver 1983), and the Ilímaussaq intrusion, South Greenland (sodalite foyaite; Δ and × are ranges in REE content of FAp; Rønsbo, 1989; Larsen 1979) (from Fleet and Pan 1997b, with permission).
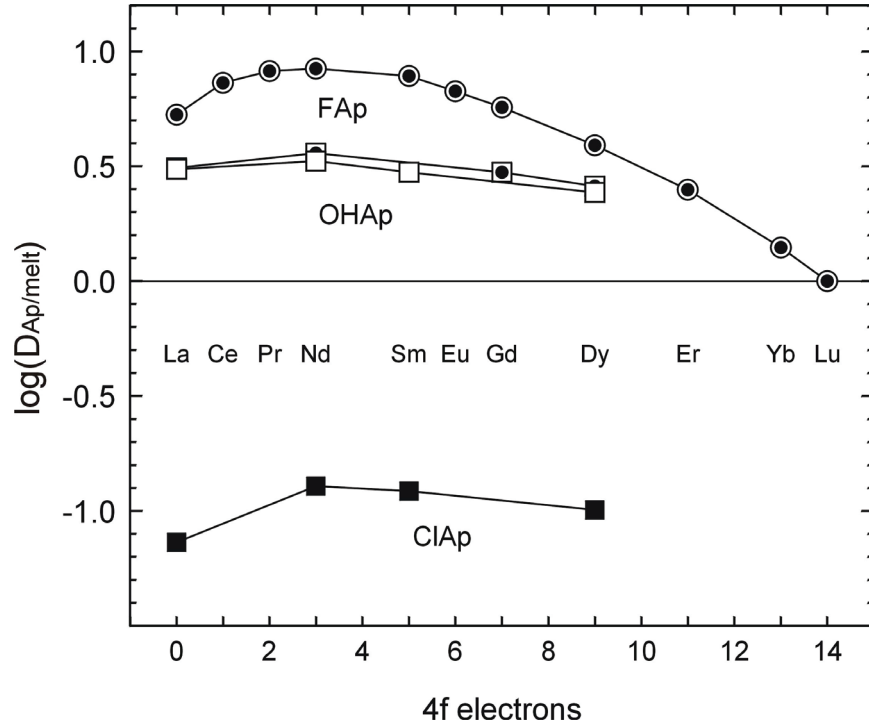
Figure 4. Melt-normalized REE contents of apatites synthesized from H_2O-bearing phosphate melts: REE-ClAp (Fleet et al. 2000a; ■); REE-FAp (Fleet and Pan 1995a; □ with central dot; Fleet and Pan 1997b, minor contents of REE; ◖ with central dot; REE-OHAp (Fleet et al. 2000b; □) (from Fleet et al. 2000a, with permission).

(Fleet et al. 2000a), whereas these elements in ClAp that crystallized from H_2O-bearing, Na-rich phosphate-chloride melts were charge-compensated by parallel substitution of Na for Ca, i.e.,

$$REE^{3+} + Na^+ = 2Ca^{2+} \qquad\qquad (10a)$$
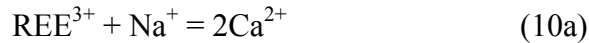
(Fleet et al. 2000b). The REEs in FAp that crystallized from H_2O-bearing phosphate-fluoride melts were charge-compensated by concomitant substitutions of both Si for P and Na for Ca (Fleet and Pan 1997b). Fleet et al. (2000b) noted that the site occupancy ratio of REE (i.e., REE-Ca2/REE-Ca1) in these synthetic apatites broadly correlated with substitution mechanism: e.g., for La-doped apatites, this ratio is 11 in OHAp (with charge compensated by Si), 4 in FAp (with charge compensated by both Si and Na), and 0.71 in ClAp (with charge compensated by Na). These observations support the suggestion of Mackie and Young (1973), who found that Nd^{3+} ions substitute for Ca in both Ca1 and Ca2 positions at approximately equal atomic proportion in NdF_3-doped FAp, but exclusively in Ca2 in Nd_2O_3-doped FAp. However, Chen et al. (2002b and Pan et al. (2002a) showed that Gd^{3+} ions in flux-grown FAp crystals containing 0.8 and 57 ppm Gd, prepared under similar conditions to those of Mackie and Young (1973), occupy both Ca1 and Ca2 sites and have Gd-Ca2/Gd-Ca1 values of 0.13 and 0.20, respectively. This marked preference of Gd for the Ca1 site in these crystals, opposite to those observed in Gd-rich Fap (e.g., Gd-Ca2/Gd-Ca1 = 2.0 for a Fap crystal containing 10.36 wt % Gd_2O_3; Fleet and Pan 1995a), is most likely attributable to the availability of intrinsic Ca^{2+} vacancies in the *c*-axis channels at ppm concentrations, i.e., via Substitution (13a) (Pan et al. 2002b). Cherniak (2000) also attributed the differences in the diffusion rates of REE in FAp among three sets of experiments (i.e., ion-implantation, in-diffusion, and out-diffusion) to differences in substitution mechanisms.

Spatial accommodation. The effect of spatial accommodation on the uptake of REE by apatites has been investigated by Fleet and Pan (1995a; 1997a) and Fleet et al. (2000a,b). It was noted that the effective size of the Ca2 site, which preferentially incorporates light REEs in FAp and OHAp, depends on the volatile anion component. Fleet et al. (2000b) showed that plots of the REE site occupancy ratio versus change in the cell volume relative to end-member structures converge toward (REE-Ca2/REE-Ca1) = 1 and $\Delta V_{unit\ cell} = 0$ for both FAp and OHAp (Fig. 5). This relationship suggests that minimization of volume strain is an important factor in the strong preference of light REEs for the Ca2 position. Ca2 is a fairly open site and readily accommodates substituents, as is evident from plots of polyhedral volume versus unit-cell volume (Fig. 6). Conversely, the individual Ca2-O distances and Ca1 polyhedral volume do not change homogeneously with change in unit-cell volume. Fleet et al. (2000b) suggested that the Ca1 polyhedron, a distorted trigonal prism, does not readily accommodate cations that are either appreciably larger or smaller than Ca2. Thus, the REE site-occupancy ratio decreases monotonically for FAp through the range of 4*f* series in response to progressive minimization of volume strain. A similar behavior is observed for OHAp, except that somewhere beyond Sm, the REE^{3+} cations become too small for strain-free substitution into Ca1 and preferentially enter Ca2. Also, uptake is optimized for $Nd^{3+} \rightarrow Gd^{3+}$, because these cations fit most readily into the Ca positions of FAp and OHAp, although this explanation appears to be more quantitative for OHAp than for FAp. The unusual site preference of REEs in ClAp also has been attributed to the large increase in size (6-8%) and distortion of the $Ca2O_6X$ polyhedron on substitution of Cl for (F,OH) (Fleet et al. 2000b).

Equalization of bond valence. Bond valence is a measure of the bonding power of an atom and is calculated using empirical bond strength-bond length correlations (Brown 1981). It has been used extensively to understand the site preference of REEs in apatites and calc-silicate minerals (Hughes et al. 1991b; Fleet and Pan 1995a,b; Pan and Fleet 1996a; Fleet et al. 2000a; Rakovan and Hughes 2000). Ca2 is the only Ca position coordinated to the volatile
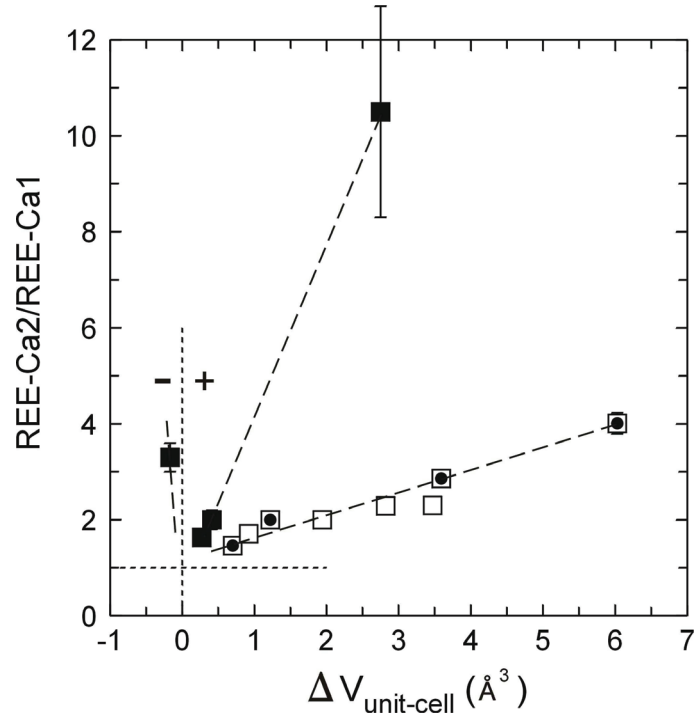
Figure 5. REE site-occupancy ratio (REE-Ca2/REE-Ca1) of REE-OHAp (Fleet et al. 2000b; ■) and REE-FAp (Fleet and Pan 1995a, □ with central dot; Fleet and Pan 1997a, □) compared with change in unit-cell volume relative to end-member OHAp and (F,OH)Ap solid solution, respectively. Note that plots reveal no site preference for REE at $\Delta V_{unit\ cell} = 0$ (from Fleet et al. 2000b, with permission).
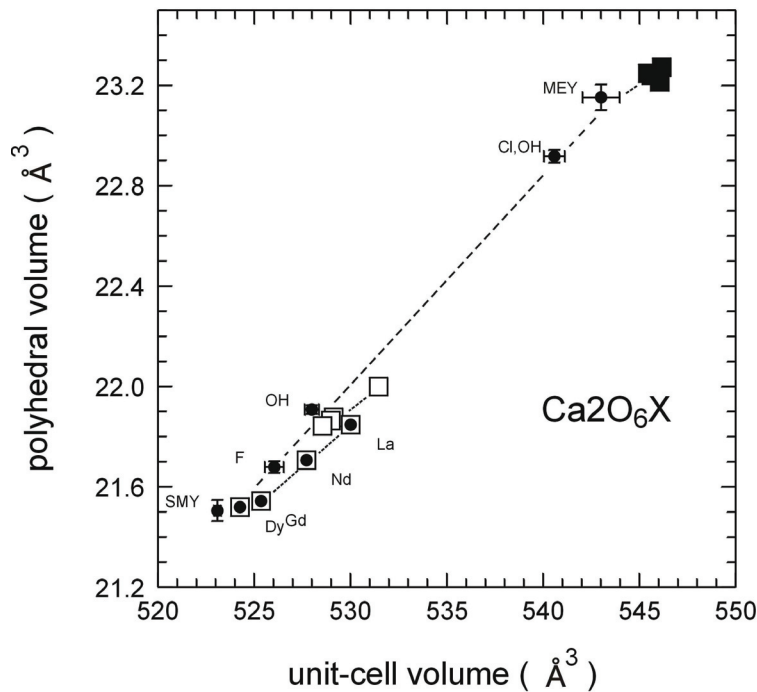
Figure 6. Variation in volume of $Ca2O_6X$ polyhedron with unit-cell volume for REE-ClAp (Fleet et al. 2000a; ■), REE-FAp (Fleet and Pan 1995a, □ with central dot); REE-OHAp (Fleet et al. 2000b, □), and synthetic (Sudarsanan et al. 1972, SMY; Mackie et al. 1972, MEY) and natural (Hughes et al. 1989) FAp, OHAp and (Cl,OH)Ap (●): trend lines have been fitted visually (from Fleet et al. 2000a, with permission).

anion component (F, OH, and Cl) and is underbonded in FAp. Therefore, Fleet and Pan (1995b) suggested that minor amounts of trivalent REEs in FAp should favor Ca2 over Ca1 to increase the bond valences of both Ca2 and F. Hughes et al. (1991b) used calculated bond valence to show that HREEs (Gd to Lu) are underbonded in both Ca positions, whereas La, Ce and Pr are slightly overbonded in the Ca1 position and therefore should prefer Ca2. Promethium and Sm should favor Ca1, and Nd should readily substitute into either Ca1 or Ca2. These results suggested that bond valence might influence both REE site preference and selectivity of apatites for REEs. However, X-ray structure refinements (Fleet and Pan 1995a; 1997a; Fleet et al. 2000a,b) revealed an apparent monotonic decrease in REE site-occupancy ratio (REE-Ca2/REE-Ca1) through the $4f$ transition-metal series, with the bond valences of Ca1 and Ca2 remaining more or less equal. In contrast, the melt-normalized REE patterns for synthetic FAp peaked near Nd-Sm (Fig. 2). These observations led Fleet and Pan (1997a) to suggest that the overall site preference for REEs is determined by equalization of bond valence but that the effective size of the Ca positions (as discussed above) exerts greater control on the selectivity of apatites for REEs. Rakovan and Hughes (2000) also extended the bond-valence requirement to explain the observed site occupancies of Sr and REEs in belovite-(Ce). They suggested that Sr, which is overbonded in the Ca1 site of FAp by as much as 0.97 valence units (Hughes et al. 1991a), competes for the Ca2 site and preferentially occupies a Ca2 site, forcing the REEs into a Ca1 equivalent site.

Crystal field contribution. Fleet et al. (2000b) noted that progressive change in individual Ca-O bond distances and O-Ca-O bond angles with substitution of REE for Ca in apatites is not continuous but tends to hinge at Nd. For example, the changes in the Ca2-O1 distance in REE-doped FAp, OHAp and ClAp all show anomalous contraction at Nd (Fig. 7). In particular, incorporation of Nd into ClAp resulted in a marked decrease in the Ca2-O1 distance, even though this element was present in greater abundance than neighboring REE cations (La and Sm). Clearly, the anomalies at Nd are not consistent with the incorporation of spherical, hard-shell cations of progressively increasing (or decreasing) radius. Fleet et al. (2000b) suggested that Nd imposes a local Jahn-Teller distortion on the Ca2 position. The $4f$ crystal field effect should be stronger for the Ca2 position because of its asymmetrical crystal field, more pronounced for Pr and Nd than adjacent REEs and heavy REEs, and absent for La, Gd and Lu (e.g., Morss 1976). This interpretation is analogous to that of Hughes et al. (1993), who suggested that the strong preference of Fe^{2+} for the Ca2 equivalent positions of a monoclinic, Fe-bearing FAp resulted from a contribution by the $3d$ crystal field stabilization energy (CFSE; cf. Burns 1993). It is noteworthy that Co^{2+} and Cr^{3+} ions have large CFSEs in asymmetrical crystal fields (Burns 1993) and therefore are expected to preferentially occupy the distorted Ca2 sites, consistent with results from X-ray structure refinements of synthetic Co and Cr-bearing apatites (Maunaye et al. 1976; Anderson and Kostiner 1987). Mn^{2+} ions of the high-spin configuration have zero CFSE, and, therefore, are controlled largely by geometric factors, and hence prefer the Ca1 position (Hughes et al. 1991a).

External (P-T-X) controls

Watson and Green (1981) reported that the partition coefficients of REEs [D(REE)] between FAp and silicate melts increase systematically with decrease in temperature and with increase in the SiO_2 content of the melt. Also, Khudolozhkin et al. (1973b) showed that the site preference of REEs for Ca2 in the FAp-britholite series decreases with increase in both temperature and content of Si, approaching zero as P is completely replaced. Similarly, Chen et al. (2002b) noted that the Gd site-occupancy ratios (Gd-Ca2/Gd-Ca1) of FAp grown in CaF_2-rich melts at 1220ºC and atmospheric pressure are significantly lower than that of a Gd-rich FAp synthesized hydrothermally at 700ºC and 0.12 GPa (Fleet and Pan 1995a). These results point to possible geothermometric applications using the intracrystalline partitioning of REEs in apatites. However, further

studies are needed to quantitatively isolate the effect of temperature from those of other factors (e.g., substitution mechanisms) on the REE site-occupancy ratios in apatites.

Chen et al. (2002b) noted that the Gd site-occupancy ratios (Gd-Ca2/Gd-Ca1) of FAp grown in CaF_2-rich melts at 1220°C and atmospheric pressure are significantly lower than that of a Gd-rich FAp synthesized hydrothermally at 700°C and 0.12 GPa (Fleet and Pan 1995a). These results point to possible geothermometric applications using the intracrystal-line partitioning of REEs in apatites. However, further studies are needed to quantitatively isolate the effect of temperature from those of other factors (e.g., substitution mechanisms) on the REE site-occupancy ratios in apatites.
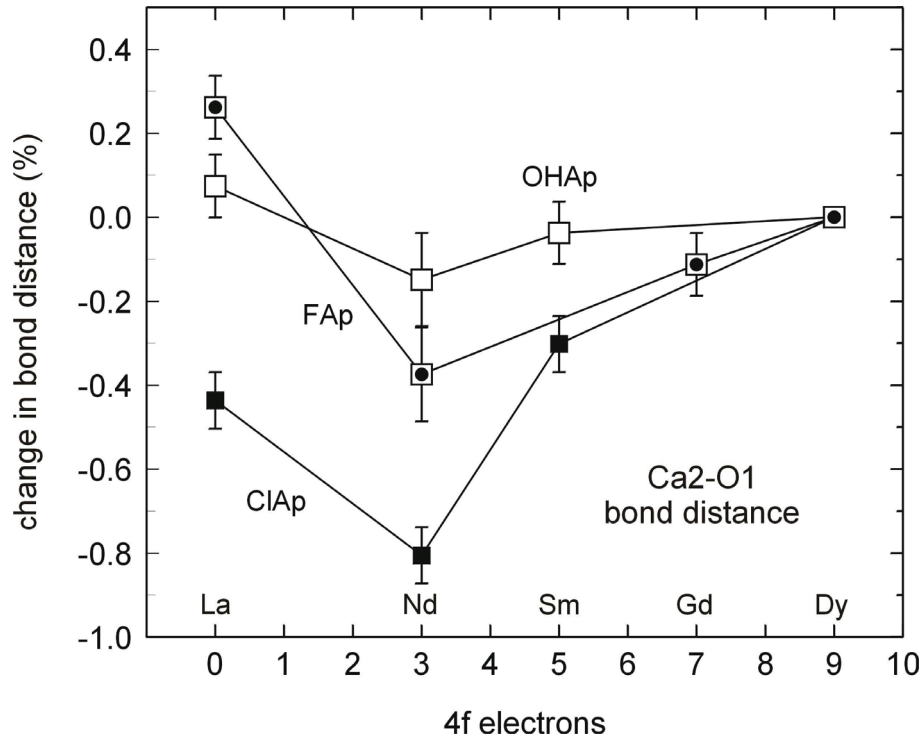
Figure 7. Change in Ca2-O1 bond distance of REE-substituted apatites with substitution of REE relative to Dy-Ap, showing anomalous decrease at Nd attributed to a *4f* crystal field contribution (from Fleet et al. 2000a, with permission).

Jolliff et al. (1993) attributed the very low apparent values of D(REE-FAp/melt) in whitlockite-bearing lunar rocks to the high temperatures expected for lunar magmas and somewhat low SiO_2 and Na_2O contents. They also noted that other melt components could be contributing factors as well, citing the positive correlation between REE abundances and content of Cl reported by Murrell et al. (1984) for FAp coexisting with whitlockite. A control on the REE uptake in FAp by melt/fluid compositions is evident in Pan and Breaks (1997), who reported marked discontinuities at Nd and Er on chondrite-normalized REE patterns of FAp from rare-element mineralized pegmatites. These discontinuities are attributed to depletion of these two elements relative to neighboring REEs in the residual melts, probably related to extreme fractionation involving monazite and garnet.

The dependence of D(REE) on SiO_2 content is generally attributed to a decrease in the number of melt sites suitable for REE^{3+} cations with increase in the degree of polymerization (Watson 1976; Ellison and Hess 1989; Gaetani and Grove 1995). Also, an increase in SiO_2 content in the melt is expected to promote the coupled substitution:

$$REE^{3+} + SiO_4^{4-} = Ca^{2+} + PO_4^{3-} \qquad (12a)$$
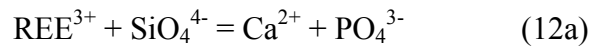
further enhancing D(REE) values. Similarly, activities of other impurities (e.g., Na) in the melt/fluid are also expected to affect the uptake of REEs by apatites because they participate directly in coupled substitutions for the incorporation of REEs into apatites (see above).

Oxygen fugacity is expected to exert direct controls on the uptake of Ce and Eu in apatites, because these two REEs commonly occur in mixed valences (e.g., Rakovan et al. 2001). Similarly, many other elements are known to be multi-valent in apatites (e.g., Cr, +3, +5 and +6; Mn, +2, +5 and +6; and S, -2 and +6) and, therefore, are expected to be influenced by oxygen fugacity. For example, the experimental data of Peng et al. (1997) revealed a correlation between the SO_3 content of FAp and fO_2, signifying a strong control on the uptake of S by fO_2.

SUMMARY AND SUGGESTIONS FOR FUTURE RESEARCH

Available data from natural occurrences and synthetic materials have shown that apatites are capable of accommodating a large number of elements and molecules because of the remarkable tolerance of these phases to structural distortion and chemical substitution. The chemistry of apatites is further complicated by nonstoichiometry, order-disorder in all of the *c*-axis anion channel, tetrahedral and Ca sites, and the presence of elements with multiple valences (e.g., Cr, Eu, Mn, and S). The example on the uptake of REEs in FAp, OHAp, and ClAp showed that the complex compositional variation in apatites is controlled by both crystal-chemical and external factors.

The diverse compositions of apatites have contributed to such important applications as petrogenetic modelling in crustal-mantle studies (e.g., Watson et al. 1985; Brenan 1993; Boudreau 1995; Pan and Fleet 1996b; Pan and Breaks 1997), paleoenvironmental reconstruction (Holmden et al. 1996, 1998; Pan and Stauffer 2000), immobilization of heavy metals (Chen et al. 1997; Arey et al. 1999) and radioactive wastes (Wronkiewicz et al. 1996), agriculture (Nriagu 1984), medical sciences (Harris et al. 2000; Kato et al. 2001) and material sciences (Steinbruegge et al. 1972; Mishra et al. 1987; Rakovan and Hughes 2000). In particular, many of these applications make direct use of specific compositional characteristics of apatites. For example, apatites as major hosts of REEs have been shown to be important in geochemical models for crustal anatexis, magma evolution and mantle compositions (Watson et al. 1985). Also, apatites with elevated Sr, REE, U, and Th contents have been widely used in radiogenic isotope analysis. In particular, the $^{87}Sr/^{86}Sr$ values of Ca apatites have long been used as a proxy of initial $^{87}Sr/^{86}Sr$ values for tracing the source and evolution of magmas and fluids, because Ca apatites typically have very low Rb/Sr values and hence relatively small amounts of radiogenic Sr from the decay of ^{87}Rb (e.g., Creaser and Gray 1992). Similarly, the compositions of biogenic apatites from fossils and sedimentary rocks have allowed a wide range of stable and radiogenic isotope (e.g., O, S, C, Sr, Nd, and U-Th-Pb) analyses with applications for environmental studies and paleoenvironmental reconstruction (Holmden et al. 1996, 1998 and references therein).

The combined geological, environmental, medical and economic importance has made apatites some of the most extensively researched minerals in the past. We have every reason to believe that these same applications and potentially new ones will attract continuing and future research on these minerals. Many applications of apatites require better understanding of their chemistry; in particular, data are generally limited or even absent for biogenic apatites due to their very fine grain size. For example, little is known about the mechanisms or rates of the uptake of REEs into biogenic apatites. Therefore, future research on factors that control on the compositions of biogenic apatites should be rewarding, because of their important applications in medical sciences, environmental studies, and paleoenvironmental reconstruction (e.g., Holmden et al. 1996, 1998; Kato et al. 2001). Similarly, the great

versatility in both structure and chemistry of apatites makes them good candidates in the quest for new and better materials, including biomaterials. For example, carbonate-bearing OHAp has been investigated extensively for its nucleation and interactions with organic molecules (e.g., proteins) in connection with its use in artificial bones (e.g., Harris et al. 2000; Kato et al. 2001; Vali et al 2001). Rakovan and Hughes (2000) suggested that it may be possible to tailor the emission characteristics of apatite hosts by controlling the distribution of activating lanthanides between the two Ca sites with specific Sr codoping. Also, Huang and Sleight (1993) showed that synthetic $Bi_2Ca_8(VO_4)_6O_2$ compound does not have a center of symmetry and therefore is a candidate for ferroelectricity.

ACKNOWLEDGMENTS

REFERENCES

Akhavan-Niaki AN (1961) Contribution a l'étude des substitutions dans les apatites. Ann Chim 6:51-79

Ames LLJr (1959) The genesis of carbonate apatites. Econ Geol 54:829-841

Anderson JB, Kostiner E (1987) The crystal structure of cobalt-substituted calcium chlorapatite. J Solid State Chem 66:343-349

Anovitz LM, Hemingway BS (1996) Thermodynamics of boron minerals: Summary of structural, volumetric and thermochemical data. Rev Mineral 33:181-261

Arden KM, Halden NM (1999) Crystallization and alteration history of britholite in rare-earth-element-enriched pegmatitic segregations associated with the Eden Lake Complex, Manitoba, Canada. Can Mineral 37: 1239-1253

Arey JS, Seaman JC, Bertsch PM (1999) Immobilization of uranium in contaminated sediments by hydroxyapatite addition. Environ Sci Tech 33:337-342

Armbruster T, Kohler T, Libowiitzky E, Friedrich A, Miletich R, Kunz M, Medenbach O, Gutzmer J (2001) Structure, compressibility, hydrogen bonding, and dehydration of the tetragonal Mn^{3+} hydrogarnet, henritermiertite. Am Mineral 86:147-158

Audubert F, Savariault JM, Lacout JL (1999) Pentalead tris(vanadate) iodide, a defect vanadinite-type compound. Acta Crystallogr C55:271-273

Ayers JC, Watson EB (1993) Apatite/fluid partitioning of rare earth elements and strontium: Experimental results at 1.0 GPa and 1000°C and application to models of fluid-rock interaction. Chem Geol 110:299-314

Azimov SY, Ismatov AA, Fedorov NF (1981) Synthetic silicophosphates, silicovanadates and silicoarsenates with the apatite structure. Inorg Mater 17:1384-1387

Bacquet G, Vo QT, Bonel G, Vignoles M (1980) Résonance paramagnétique élétronique du centre F^+ dans les fluorapatites carbonatées de type B. J Solid State Chem 33:189-195

Bacquet G, Vo QT, Vignoles M, Bonel G (1981a) EPR detection of acetate ions trapping in B-type carbonated fluorapatites. J Solid State Chem 39:148-153

Bacquet G, Vo QT, Vignoles M, Bonel G (1981b) ESR of the F^+ centre in B-type carbonated hydroxyapatite. Phys Status Solidi 68:71-74

Banks E, Greenblatt M, McGarvey BR (1971) Electron spin resonance of CrO_4^{3-} in chlorapatite $Ca_5(PO_4)_3Cl$. J Solid State Chem 3:308-313

Banks E, Jaunarajs KL (1965) Chromium analogs of apatite and spodiosite. Inorg Chem 4, 78-83

Baran EJ, Baud G, Besse J-P (1983) Vibrational spectra of some rhenium-apatites containing ReO_5-groups. Spectrochim Acta 39A:383-386

Baud G, Besse J-P, Sueur G, Chevalier R (1979) Structure de nouvelles apatites au rhenium contenant des anions volumineux: $Ba_{10}(ReO_5)_6X_2$ (X = Br,I). Mater Res Bull 14:675-682

Baud G, Besse J-P, Capestan M, Sueur G, Chevalier R (1980) Étude comparative d'apatites contenant I'ion $(ReO_5)^{3-}$. Structure des fluoro et carbonatoapatites. Ann Chim Sci Mater 5:575-583

Baumer A, Caruba R, Bizzouard H, Peckett A (1983) Chlorapatite de synthésis: substitution et inclusions de Mn, Ce, U et Th traces. Can Mineral 21:567-573

Baumer A, Caruba R, Ganteaume M (1990) Carbonate-fluorapatite: Mise en évidence de la substitution 2 $PO_4^{3-} \rightarrow SiO_4^{4-} + SO_4^{2-}$ par spectrométrie infrarouge. Eur J Mineral 2:297-304

Berndt ME, Seyfried WEJr (1997) Calibration of Br/Cl fractionation during phase separation of seawater: Possible halite at 9 to 10°N East Pacific Rise. Geochim Cosmochim Acta 61:2849-2854

Beshah K, Rey C, Glimcher MJ, Schimizu M, Griffin RG (1990) Solid state carbon-13 and proton NMR studies of carbonate-containing calcium phosphates and enamel. J Solid State Chem 84:71-81

Besse J-P, Baud G, Levasseur G, Chevallier R (1979) Structure crystalline de $Ba_5(ReO_5)_3Cl$: une nouvelle apatite contenant l'ion $(ReO_5)^{3-}$. Acta Crystallogr B35:1756-1759

Besse J-P, Baud G, Chevallier R, Zarembowitch J (1980) Mise en évidence de l'ion O_2^- dans l'apatite au rhénium $Ba_5(ReO_5)_3O_2$. Mater Res Bull 15:1255-1261

Bigi A, Foresti E, Marchetti F, Ripamonti A, Roveri N (1984) Barium calcium hydroxyapatite solid solutions. J Chem Soc Dalton Trans, p 1091-1093

Bigi A, Gazzano M, Ripamonti A, Foresti E, Roveri N (1986) Thermal stability of cadmium-calcium hydroxyapatite solid solutions. J Chem Soc Dalton Trans, p 241-244

Bigi A, Falini G, Gazzano M, Roveri N, Tedesco E (1998) Structural refinements of strontium substituted hydroxyapatites. Mater Sci Forum 278:814-819

Binder G, Troll G (1989) Coupled anion substitution in natural carbon-bearing apatites. Contrib Mineral Petrol 101:394-401

Böhlke JK, Irwin JJ (1992) Laser microprobe analysis of Cl, Br, I and K in fluid inclusions: Implications for sources of salinity in some hydrothermal fluids. Geochim Cosmochim Acta 56:203-225

Bonel G (1972) Contribution a l'étude de la carbonatation des apatites: I. Ann Chim 7:65-87

Bonel G, Montel G (1964) Sur une nouvelle apatite carbonatée synthétique. Compt Rend Acad Sci 258:923-926

Bonel G, Labarthe JC, Vignoles C (1973) Contribution a l'étude structurale des apatitescarbonatees de type B. Colloq Intern CNRS 230:117-125

Bonel G, Heughebaert J-C, Hughebaert M, Lacout JL, Lebugle A (1988) Apatitic calciumorthophosphates and related compounds for biomaterials preparation. Ann New York Acad Sci 523:115-130

Borisov SV, Klevtsova RF (1963) The crystal structure of REE-Sr apatite. Zh Struct Khim 4:629-631

Borneman-Starynkevich ID (1938) On some isomorphic substitutions in the apatite group. Dokl Akad Nauk SSSR 19:253-255

Borneman-Starynkevich ID, Belov NV (1953) Carbonate-apatites. Doklad Akad Nauk SSSR 90:89-92

Bothe JV Jr, Brown PW (1999) Arsenic immobilization by calcium arsenate formation. Environ Sci Tech 33:3806-3811

Boudreau AE (1995) Fluid evolution in layered intrusions: Evidence from the chemistry of halogen-bearing minerals. *In* Magmas, Fluids, and Ore Deposits. Thompson JFH (ed) Mineral Assoc Can Short Course Series 23:25-45

Brasseur H, Dallmagne MJ (1949) Stnthèse de l'apatites. Bull Soc Chim France 135-137

Brenan JM (1993) Partitioning of fluorine and chlorine between apatite and aqueous fluids at high pressure and temperature: Implications for the F and Cl contents of high P-T fluids. Earth Planet Sci Lett 117:251-263

Brophy GP, Nash JT (1968) Compositional, infrared, and X-ray analysis of fossil bone. Am Mineral 53: 445-454

Brown ID (1981) The bond-valence method: An empirical approach to chemical structure and bonding. *In* Structure and Bonding in Crystals. O'Kieffe M, Navrotsky A (eds) Academic Press, p 1-30

Burns RG (1993) Mineralogical Applications of Crystal Field Theory (2nd edn). Cambridge University Press, Cambridge, UK

Buvaneswari G, Varadaraju UV (2000) Synthesis and characterization of new apatite-relatedphosphates. J Solid State Chem 149:133-136

Calvo C, Faggiani R, Krishnamachari N (1975) Crystal structure of $Sr_{9.402}Na_{0.209}(PO_4)_6B_{0.996}O_2$—a deviant apatite. Acta Crystallogr B31:188-192

Cavaretta G, Mottana A, Tecce E (1981) Cesanite, $Ca_2Na_3[(OH)(SO_4)_3]$, a sulfate isotypic to apatite from the Cesano geothermal field (Latium Italy). Mineral Mag 44:269-273

Chakhmouradian A, Reguir E, Mitchell R (2002) Strontium-apatite: New occurrences and the extent of Ca-Sr substitution in apatite-group minerals. Can Mineral 40:121-136

Chen N, Pan Y, Weil JA (2002a) Electron paramagnetic resonance spectroscopic study of synthetic fluorapatite: Part I. Local structural environment and substitution mechanism of Gd at the Ca2 site. Am Mineral 87: 37-46

Chen N, Pan Y, Weil JA, Nilges MJ (2002b) Electron paramagnetic resonance spectroscopic study of synthetic fluorapatite: Part II. Gd^{3+} at the Ca1 site, with a neighboring Ca2 vacancy. Am Mineral 87:47-55

Chen N, Pan Y, Weil JA, Nigles MJ (2002c) EPR study of ^{157}Gd-doped fluorapatite: Hyperfine and nuclear quadrupole splitting anisotropy. Geol Assoc Can Mineral Assoc Can Abstr 27:19-20

Chen XB, Wright J, Conca I, Peurrung LM (1997) Evaluation of heavy metal remediation using mineral apatite. Water Air Soil Pollut 98:57-78

Cherniak DJ (2000) Rare earth element diffusion in apatite. Geochim Cosmochim Acta 64:3871-3885

Chesnokov BV, Bazhenova LF, Bushmakin AF (1987) Fluorellestadite $Ca_{10}[(SO_4),(SiO_4)]_6F_2$—a new mineral. Zap Vser Mineral Obsh 1167:743-746

Chiranjeevirao SV, Hemmerle J, Voegel JC, Frank RM (1982) A method of preparation and characterization of magnesium-apatites. Inorg Chim Acta 67:183-187

Cho G, Yesinowski JP (1993) Multiple-quantum NMR dynamics in the quasi-one-dimensional distribution of protons in hydroxyapatite. Chem Phys Lett 205:1-5

Cho G, Yesinowski JP (1996) ^{1}H and ^{19}F multiple-quantum NMR dynamics in quasi-one-dimensional spin clusters in apatites. J Chem Phys 100:15716-15725

Christy AG, Alberius-Henning P, Lidin SA (2001) Computer modelling and description of nonstoichiometric apatites $Cd_{5-/2}(VO_4)_3I_{1-}$ and $Cd_{5-/2}(PO_4)_3Br_{1-}$ as modified chimney-ladder structures with ladder-ladder and chimney-ladder coupling. J Solid State Chem 156:88-100

Clarke RS, Altschuler ZS (1958) Determination of the oxidation state of uranium in apatite and phosphorite deposits. Geochim Cosmochim Acta 13:127-142

Cockbain AG, Smith GV (1967) Alkaline-earth – rare-earth silicate and germanate apatites. Mineral Mag 36:411-421

Comodi P, Liu Y, Stoppa F, Woolley AR (1999) A multi-method analysis of Si-, S- and REE-rich apatite from a new kind of kalsilite-bearing leucitite (Abruzzi, Italy). Mineral Mag 63:661-672

Creaser RA, Gray CM (1992) Preserved initial [87]Sr/[86]Sr in apatites from altered felsic igneous rocks: A case study from the Middle Proterozoic of South Australia. Geochim Cosmochim Acta 56:2789-2795

Dai Y, Hughes JM (1989) Crystal structure refinements of vanadinite and pyromorphite. Can Mineral 27: 189-192

Dai Y, Hughes JM, Moore PB (1991) The crystal structure of mimetite and clinomimetite, $Pb_5(AsO_4)_3Cl$. Can Mineral 29:369-376

Davis TS, Kreidler ER, Parodi JA, Soules TF (1971) The luminescent properties of antimony in calcium halophosphates, J Lumines 4:48-62

DeBoer BG, Sakthivel A, Cagle JR, Young RA (1991) Determination of the antimony substitution site in calcium fluorapatite from powder X-ray diffraction data. Acta Crystallogr B47:683-692

Deganello S (1983) The crystal structure of ceanite at 21 and 236°C. N Jahrb Mineral Monatsh 305-313

Della-Ventura G, Williams CT, Cabella R, Oberti R, Caprilli E, Bellatreccia F (1999) Britholite-hellandite intergrowths and associated REE-minerals from he alkali-syenitic ejecta of the Vico volcanic complex (Latium, Italy): petrological implications bearing on REE mobility in volcanic systems. Eur J Mineral 11:843-854

Doi Y, Moriwaki Y, Aoba T, Takahashi J, Joshin K (1982) ESR and IR studies of carbonate-containing hydroxyapatites. Calcif Tissue Intl 34:178-181

Dong P, Pan Y (2002) F-Cl-Br partitioning between apatites and halide-rich melts: Experimental studies and applications. Geol Ass Can Mineral Ass Can Abstr 27:29

Dowker SEP, Elliott JC (1983) Infrared study of the formation, loss and location of cyanate and cyanamide in thermally treated apatites. J Solid State Chem 49: 334-340

Dugas J, Rey C (1977) Electron spin resonance characterization of superoxide ions in some oxygenated apatites. J Phys Chem 81:1417-1419

Dugas J, Bejjaji B, Sayah D, Trombe JC (1978) Etude par RPE de l'ion NO_2^{2-} dans une apatite nitrée. J Solid State Chem 24:143-151

Dunn PJ, Rouse RC (1978) Morelandite, a new barium arsenate chloride member of the apatite group. Can Mineral 16:601-604

Dunn PJ, Peacor DR, Newberry N (1980) Johnbaumite, a new member of the apatite group from Franklin, New Jersey. Am Mineral 65:1143-1145

Dunn PJ, Peacor DR, Valley JW, Randall CA (1985a) Ganomalite from Franklin, New Jersey, and Jakobsberg, Sweden; new chemical and crystallographic data. Mineral Mag 49:579-582

Dunn PJ, Petersen EU, Peacor DR (1985b) Turneaureite, a new member of the apatite group from Franklin, New Jersey, Balmant, New York and Laangban, Sweden. Can Mineral 23:251-254

Dupree R, Lewis MH, Smith ME (1988) High resolution silicon-29 nuclear magnetic resonance in the Y-Si-O-N system. J Am Chem Soc 110:1083-1087

Dymek RF, Owens BE (2001) Petrogenesis of apatite-rich rocks (nelsonites and oxide-apatite gabbronorites) associated with massif anorthosites. Econ Geol 96:797-815

Edgar AD (1989) Barium- and strontium-enriched apatites in lamproites from West Kimberley, Western Australia. Am Mineral 74:889-895

Efimov AS, Kravchenko SM, Vasil'eva ZV (1962) Strontium-apatite: a new mineral. Dokl Akad Nauk SSSR 142:439-442

Elliott JC (1964) The crystallographic structure of dental enamel and related apatites. PhD dissertation, University of London, London, UK

Elliott JC (1969) Recent progress in the chemistry, crystal chemistry and structure of the apatites. Calcif Tissue Res 3:293-307

Elliott JC (1994) Structure and Chemistry of the Apatites and Other Calcium Orthophosphates. Elsevier, Amsterdam

Elliott JC, Mackie PE, Young RA (1973) Monoclinic hydroxyapatite. Science 180:1055-1057

Elliott JC, Bonel G, Trombe JC (1980) Space group and lattice constants of $Ca_{10}(PO_4)_6CO_3$. J Appl Crystallogr 13:618-621

Elliott JC, Dykes E, Mackie PE (1981) Structure of bromapatite, $Ca_5(PO_4)_3Br$, and the radius of the bromide ion. Acta Crystallogr B37:435-438

Ellison AJG, Hess PC (1989) Solution properties of rare earth elements: Inference from immiscible liquids. Geochim Cosmochim Acta 53:1965-1974

Engel G (1970) Hydrothermal synthese von bleihyoxylapatiten $Pb_5(XO_4)_3OH$ mit X = P, As, V. Naturwissen-schaften 57:355

Engel G (1973) Infrarotspektroskopische und röntgenographische untersuchungen von bleihydorxylapatit, bleioxyapatit und bleialkaliapatit. J Solid State Chem 6:286-292

Engel G (1978) Fluoroberyllate mit apatitstruktur und ihre beziehungen zu sulfaten und silicaten. Mater Res Bull 13:43-48

Engel G, Kreig F, Reif G (1975) Mischekristallbildung und kationeordnung im system bleihydroxylapatit-calciumhydroxylapatit. J Solid State Chem 15:117-126

Ercit TS, Cerny P, Groat LA (1994) The crystal structure of Mn-rich fluorapatite and the role of Mn in the apatite structure. Geol Assoc Can Mineral Ass Can Abstr 19:A34

Fayos J, Watkin DJ, Pérez-Méndez M (1987) Crystal structure of the apatite-like compound $K_3Ca_2(SO_4)_3F$. Am Mineral 72:209-212

Felsche F (1972) Rare earth silicates with apatite structure. J Solid State Chem 5:266-275

Fleet ME, Pan Y (1994) Site preference of Nd in fluorapatite $[Ca_{10}(PO_4)_6F_2]$. J Solid State Chem 111:78-81

Fleet ME, Pan Y (1995a) Site preference of rare earth elements in fluorapatite. Am Mineral 80:329-335

Fleet ME, Pan Y (1995b) Crystal chemistry of rare earth elements in fluorapatite and calc-silicate minerals. Eur J Mineral 7:591-605

Fleet ME, Pan Y (1997a) Site preference of rare earth elements in fluorapatite: Binary (LREE+HREE)-substituted crystals. Am Mineral 82:870-877

Fleet ME, Pan Y (1997b) Rare earth elements in apatite: Uptake from H_2O-bearing phosphate-fluoride melts and the role of volatile components. Geochim Cosmochim Acta 61:4745-4760

Fleet ME, Liu X, Pan Y (2000a) Rare earth elements in chlorapatite $[Ca_{10}(PO_4)_6Cl_2]$: Uptake, site preference and degradation of monoclinic structure. Am Mineral 85:1437-1446

Fleet ME, Liu X, Pan Y (2000b). Site preference of rare earth elements in hydroxyapatite $[Ca_{10}(PO_4)_6(OH)_2]$. J Solid State Chem 149:391-398

Fleischer M, Altschuler ZS (1986) The lanthanides and yttrium in minerals of the apatite group – an analysis of the available data. N Jahrb Mineral Monatsh 467-480

Fleischer M, Mandarino JA (1995) Glossary of Mineral Species (7th ed). Mineral Record, Tucson, Arizona.

Förtsch E, Freiburg IB (1970) Untersuchungen as mineralien der pyromorphit gruppe. N Jahrb Mineral Abh 113:219-250

Fowler BO (1974) Infrared studies of apatites. II. Preparation of normal and isotopically substituted calcium, strontium, and barium hydroxyapatite and spectra-structure-composition-correlations. Inorg Chem 13: 207-214

Fransolet A-M, Schreyer W (1981) Unusual, iron-bearing apatite from a garnetiferous pegmatoid, Northampton Block, Western Australia. N Jahrb Mineral Monatsh 317-327

Frondel C, Ito J (1957) Geochemistry of germanium in the oxidized zone of the Tsumeb Mine, South-West Africa. Am Mineral 42:743-753

Gaetani GA, Grove TL (1995) Partitioning of rare earth elements between clinopyroxene and silicate melt: Crystal-chemical controls. Geochim Cosmochim Acta 59:1951-1962

Gaft M, Reisfeld DR, Ranczer G, Shoval S, Champagnon B, Boulon G (1997) Eu^{3+} luminescence in high-symmetry sites of natural apatite. J Lumines 72-74:572-574

Gaudé J, L'Haridon P, Hamond C, Marchand R, Laurent Y (1975) Composés à structure apatite. I. Structure de l'oxynitrure $Sm_{10}Si_6N_2O_{24}$. Bull Soc fr Minéral Cristal 98:214-217

Giuseppetti G, Rossi G, Tadini C (1971) The crystal structure of nasonite. Am Mineral 56:1174-1179

Grandjean-Lécuyer P, Feist R, Albarède F (1993) Rare earth elements in old biogenic apatites. Geochim Cosmochim Acta 57:2507-2514

Grisafe DA, Hummel FA (1970) Crystal chemistry and color in apatites containing cobalt, nickel and rare-earth ions. Am Mineral 55:1131-1145

Gromet L P, Silver LT (1983) Rare earth element distributions among minerals in a granodiorite and their petrogenic implications. Geochim Cosmochim Acta 47:925-939

Gruner JW, McConnell D (1937) The problem of the carbonate-apatites. Z Krist 97A:208-215

Guyader J, Grekov FF, Marchand R, Lang J (1978) Nouvelles séties de silicoapatites enrichies en azote. Rev Chim Minéral 15:431-438

Harada K, Nagashima K, Nakao K, Kato A (1971) Hydroxylellestadite, a new apatite from Chichibu mine, Saitama Prefecture, Japan. Am Mineral 56:1507-1518

Harries JE, Hasnain SS, Shah JS (1987) EXAFS study of structural disorder in carbonate-containing hydroxyapatite. Calcif Tissue Intl 41:346-350

Harris NL, Rattray KR, Tye CE, Underhill TM, Somerman MJ, D'Errico JA, Chambers AF, Hunter GK, Goldberg HA (2000) Functional analysis of bone sialoproteIn Identification of the hydroxyapatite-nucleating and cell-binding domains by recombinant peptide expression and site-directed mutagenesis. Bone 27:795-802

Harris RK, Leach MJ, Thompson DP (1989) Silicon-29 magic-angle spinning nuclear magnetic resonance study of some lanthanum and yttrium silicon oxynitride phases. Chem Material 1:336-338

Hata M, Marumo F, Iwai S, Aoki H (1979) Structure of barium chlorapatite. Acta Crystallogr B35:2382-2384

Hata M, Marumo F, Iwai S, Aoki H (1980) Structure of a lead apatite $Pb_9(PO_4)_6$. Acta Crystallogr B36: 2128-2130

Hata M, Okada K, Iwai S, Akao M, Aoki H (1978) Cadmium hydroxyapatite. Acta Crystallogr B34:3062-3064

Heijligers HJM, Verbeeck RMH, Driessens FCM (1979) Cation distribution in calcium-strontium-hydroxyapatites. J Inorg Nuclear Chem 41:763-764

Hitmi N, LaCabanne C, Bonel G, Roux P, Young RA (1986) Dipole co-operative motions in an A-type carbonated apatite, $Sr_{10}(AsO_4)_6CO_3$. J Phys Chem Solids 47:507-515

Hogarth DD, Staecy HR, Semenov EI, Proshchenko EG, Kazakova ME, Kataeva ZT (1973) New occurrences and data of spencite. Can Mineral 12:66-71

Holmden C, Creaser RA, Muehlenbachs K, Leslie SA, Bergstrom SM (1996) Isotopic and elemental systematics of Sr and Nd in 454 Ma biogenic apatites: Implications for paleoseawater studies. Earth Planet Sci Lett 142:425-437

Holmden C, Creaser RA, Muehlenbachs K, Leslie SA, Bergstrom SM (1998) Isotopic evidence for geochemical decoupling between epeiric seas and bordering oceans: Implications for secular curves. Geology 26:567-570

Hounslow AW, Chao GY (1970) Monoclinic chlorapatite from Ontario. Can Mineral 10:252-259

Huang J, Sleight AW (1993) The apatite structure without an inversion center in a new bismuth calcium vanadium oxide $BiCa_4V_3O_{13}$. J Solid State Chem 104:52-58

Hughes JM, Cameron M, Crowley KD (1989) Structural variations in natural F, OH, and Cl apatites. Am Mineral 74:870-876

Hughes JM, Cameron M, Crowley KD (1990) Crystal structures of natural ternary apatites: solid solutions in the $Ca_5(PO_4)_3X$ (X=F, OH, Cl) system. Am Mineral 75:295-304

Hughes JM, Cameron M, Crowley KD (1991a) Ordering of divalent cations in apatite structure: crystal structure refinements of natural Mn- and Sr-bearing apatites. Am Mineral 76:1857-1862

Hughes JM, Cameron M, Mariano AN (1991b) Rare-earth element ordering and structural variations in natural rare-earth-bearing apatite. Am Mineral 76:1165-1173

Hughes JM, Drexler JW (1991) Cation substitution in the apatite tetrahedral site: crystal structures of type hydroxylellstadite and type fermorite. N Jahrb Mineral Monatsh 327-336

Hughes JM, Fransolet A-M, Schreyer W (1993) The atomic arrangement of iron-bearing apatite. N Jahrb Mineral Monatsh 504-510

Hughes JM, Mariano AN, Drexler JW (1992) Crystal structures of synthetic Na-REE-Si oxyapatites, synthetic monoclinic britolite. N Jahrb Mineral Monatsh 311-319

Hughson MR, Sen Gupta JG (1964) A thorian intermediate member of the britholite-apatite series. Am Mineral 49:937-951

Ikoma T, Yamazaki A, Nakamura S, Akao M (1999) Preparation and structure refinement of monoclinic hydroxyapatite. J Solid State Chem 144:272-276

Ito J (1968) Silicate apatites and oxyapatites. Am Mineral 53:890-907

Ito A, Aoki H, Akao M, Miura N, Otsuka R, Tsutsumi S (1988) Structure of borate groups in borate-containing apatite. J Ceram Soc Japan 96:695-697

Ivanova TI, Frank-Kamenetskaya OV, Kol'tsov V, Ugolkov L (2001) Crystal structure of calcium-deficient carbonated hydroxyapatite. Thermal decomposition. J Solid State Chem 160:340-349

Jahnke RA (1984) The synthesis and solubility of carbonate fluorapatite. Am J Sci 284:58-78

Jolliff BL, Haskin LA, Colson RO, Wadhwa M (1993) Partitioning in REE-saturating minerals: Theory, experiment and modelling of whitlockite, apatite, and evolution of lunar residual magmas. Geochim Cosmochim Acta 57:4069-4094

Joris SJ, Amberg CH (1971) The nature of deficiency in nonstoichiometric hydroxyapatite. II. Spectroscopic studies of calcium and strontium hydroxyapatite. J Phys Chem 75:3172-3178

Kato H, Nishiguchi S, Furukawa T, Neo M, Kawanabe K, Saito K, Nakamura T (2001) Bone bonding in sintered hydroxyapatite combined with a new synthesized agent, TAK-778. J Biomed Mater Res 54:619-629

Kautz K, Gubser R (1969) Untersuchungen mit der elektronen-mikrosonde an zonargebauten mineralen der pyromorphit gruppe. Contrib Mineral Petrol 20:298-305

Khattech I, Jemal M (1997) Thermochemistry of phosphate products. II. Standard enthalpies of formation and mixing of calcium and strontium fluorapatites. Thermochim Acta 298:23-30

Khomyakov AP, Lisitsyn DV, Kulikova IM, Rastsvetayeva RK (1996) Deloneite-(Ce), $NaCa_2SrCe(PO_4)_3F$, a new mineral with a belovite-like structure. Zap Vser Mineral Obsh 125:83-94

Khorari S, Cahay R, Rulmont A, Tarte P (1994) The coupled isomorphic substitution $2(PO_4)^{3-} = (SO_4)^{2-} + (SiO_4)^{4-}$ in synthetic apatite $Ca_{10}(PO_4)_6F_2$: a study by X-ray diffraction and vibrational spectroscopy. Eur J Solid State Inorg Chem 31:921-934

Khudolozhkin VO, Urusov VS, Kurash VV (1974) Mössbauer study of the ordering of Fe^{2+} in the fluor-apatite structure. Geochem Intl 11:748-750

Khudolozhkin VO, Urusov VS, Tobelko KI (1972) Ordering of Ca and Sr in cation positions in the hydroxylapatite-belovite isomorphous series. Geochem Intl 9:827-833

Khudolozhkin VO, Urusov VS, Tobelko KI (1973a) Distribution of cations between sites in the structure of Ca, Sr, Ba - apatites. Geochem Intl 10:266-269

Khudolozhkin VO, Urusov VS, Tobelko KI, Vernadskiy VI (1973b) Dependence of structural ordering of rare earth atoms in the isomorphous series apatite-britholite (abukumalite) on composition and temperature. Geochem Intl 10:1171-1177

Kingsley JD, Prener JS, Segall B (1965) Spectroscopy of $(MnO_4)^{3-}$ in calcium halophosphates. Phys Rev A137:189-202

Klement R, Haselbeck H (1965) Apatite and wagnerite zweiwertige metalle. Z Anorg Allgem Chem 336: 113-128

Kreidler ER, Hummel FA (1970) The crystal chemistry of apatite: structure fields of fluor- and chlorapatite. Am Mineral 55:170-184

Kutoglu A von (1974) Structure refinement of the apatite $Ca_5(VO_4)_3(OH)$. N Jahrb Mineral Monatsh 210-218

Labarthe J-C, Bonel G, Montel G (1971) Sur la localisation des carbonate dans le réseau des apatites calciques. Compt Rend Acad Sci 273:349-351

Labarthe J-C, Therasse M, Bonel G, Montel G (1973) Sur la structure des apatites phosphocalciques carbonatées de type B. Compt Rend Acad Sci 276:1175-1178

Lacout JL, Mikou M (1989) Sur les dioxyapatites phosphostrontiques contenant deux ions de terres rares. Ann Chim 14:9-14

Larsen L M (1979) Distribution of REE and other trace elements between phenocrysts and peralkaline undersaturated magmas, exemplified by rocks from the Gardar igneous province, south Greenland. Lithos 12:303-315

LeGeros RZ (1965) Effect of carbonate on the lattice parameters of apatite. Nature 206:403-404

Liu Y, Comodi P (1993) Some aspects of the crystal chemistry of apatites. Mineral Mag 57:709-719

Mackie PE, Elliott JC, Young RA (1972) Monoclinic structure of synthetic $Ca_5(PO_4)_3Cl$ chlorapatite. Acta Crystallogr A28:1840-1848

Mackie PE, Young RA (1973) Location of Nd dopant in fluorapatite, $Ca_5(PO_4)_3F$:Nd. J Appl Crystallogr 6: 26-31

Mathew M, Mayer I, Dickens B, Schroeder LW (1979) Substitution in barium-fluoride apatite: the crystal structures of $Ba_{10}(PO_4)_6F_2$, $Ba_6La_2Na_2(PO_4)_6F_2$ and $Ba_4La_3Na_3(PO_4)_6F_2$. J Solid State Chem 28:79-95

Mathew M, Brown WE, Austin M, Negas T (1980) Lead alkali apatites without hexad anion: the crystal structure of $Pb_8K_2(PO_4)_6$. J Solid State Chem 35:69-76

Maunaye M, Hamon C, L'Haridon P, Laurent Y (1976) Composés á structure apatite. IV. Étude structurale de l'oxynitrure $Sm_8Cr_2Si_6N_2O_{24}$. Bull Soc fr Minéral Cristal 99:203-205

Mayer I, Cohen S (1983) The crystal structure of $Ca_6Eu_2Na_2(PO_4)_6F_2$. J Solid State Chem 48:17-20

Mayer I, Roth RS, Brown WE (1974) Rare earth substituted fluoride-phosphate apatites. J Solid State Chem 11:33-37

Mayer I, Fischbein E, Cohen S (1975) Apatites of divalent europium. J Solid State Chem 14:307-312

Mayer I, Semadja A (1983) Bismuth-substituted calcium, strontium, and lead apatites. J Solid State Chem 46:363-366

Mayer I, Swissa S (1985) Lead and strontium phosphate apatites substituted by rare earth and silver ions. J Less Common Metals 110:411-414

Mazza D, Tribaudino M, Delmstro A, Lebech B (2000) Synthesis and neutron structure of $La_5Si_2BO_{13}$, an analogue of the apatite mineral. J Solid State Chem 155:389-393

McArthur MJ (1985) Francolite geochemistry-compositional controls during formation, diagenesis, metamorphism, and weathering. Geochim Cosmochim Acta 49:23-35

McConnell D (1937) The substitution of SiO_4 and SO_4 for PO_4 groups in the apatite structure; ellestadite, the end member. Am Mineral 22:977-986

McConnell D (1952) The problem of the carbonate apatites. IV. Structural substitutions involving CO_3 and OH. Bull Soc Fr Mineral Cristall 75:428-445

McConnell D (1973) Apatite. Its Crystal Chemistry, Mineralogy, Utilization, and Geologic and Biologic Occurrences. Springer, New York

Merker L, Engel G, Wondratschek H, Ito J (1970) Lead ions and empty halide sites in apatites. Am Mineral 55:1435-1436

Mishra KC, Patton RJ, Dale EA, Das TP (1987) Location of antimony in a halophosphate phosphor. Phys Rev B35:1512-1520

Mitchell L, Faust GT, Hendricks SB, Reynolds DS (1943) The mineralogy and genesis of hydroxylapatite. Am Mineral 28:356-371

Miyake M, Ishigaki K, Suzuki T (1986) Structure refinements of Pb^{2+} ion-exchanged apatites by X-ray powder pattern-fitting. J Solid State Chem 61:230-235

Mohseni-Koutchesfehani S (1961) Contribution à l'étude des apatites barytiques. Ann Chim: 463-479

Moore PB, Araki T (1977) Samuelsonite: its crystal structure and relation to apatite and octacalcium phosphate. Am Mineral 62:229-245

Moran LB, Berkowitz JK, Yeinowski JP (1992) ^{19}F and ^{31}P magic-angle spinning nuclear magnetic resonance of antimony(III)-doped fluorapatite phosphors: Dopant sites and spin diffusion. Phys Rev B45:5347-5360

Morss LS (1976) Thermochemical properties of yttrium, lanthanum, and lanthanide elements and ions. Chem Rev 76:827-841

Murrell MT, Brandriss M, Woolum DS, Burnett DS (1984) Pu-REE-Y partitioning between apatite and whitlockite. Lunar Planet Sci XV:579-580

Nadal M, LeGeros RZ, Bonel G, Montel G (1971) Mise en évidence d'un phénomène d'order-désordre dans le réseau des carbonate-apatites strontique. Compt Rend Acad Sci 272:45-48

Neuman WF, Mulryan BJ (1971) Synthetic hydroxyapatite crystals IV. Magnesium incorporation. Calcif Tissue Intl 7:133-138

Newberry NG, Essene EJ, Peacor DR (1981) Alforsite, a new member of the apatite group: The barium analogue of chlorapatite. Am Mineral 66:1050-1053

Nobes RH, Akhmatskaya EV, Milman V, White JA, Winkler B, Pickard CJ (2000) An *ab initio* study of hydrogarnets. Am Mineral 85:1706-1715

Nriagu JO (1984) Formation and stability of base metal phosphates in soils and sediments. *In* Phosphate Minerals. Nriagu JO, Moore PB (eds) Springer-Verlag, New York, p. 318-329

Oberti R, Ottolini L, Della Ventura G, Pardon GC (2001) On the symmetry and crystal chemistry of britholite: New structural and microanalytical data. Am Mineral 86:1066-1075

Ohkubo Y (1968) EPR spectra of manganese(II) ions in synthetic calcium chloride fluoride phosphates. J Appl Phys 39:5344-5345

Okazaki M (1983) $F^-CO_3^{2-}$ interactions in IR spectra of fluoridated CO_3-apatites. Calcif Tissue Intl 35:78-81

O'Reilly SY, Griffin WL (2000) Apatite in the mantle: implications for metasomatic processes and high heat production in Phanerozoic mantle. Lithos 53 217-232

Pan Y, Breaks FW (1997) Rare earth elements in fluorapatite, Separation Lake area, Ontario: Evidence for S-type granite - rare-element pegmatite linkage. Can Mineral 35:659-671

Pan Y, Chen N, Weil JA, Nilges MJ (2002a) Electron paramagnetic resonance spectroscopic study of synthetic fluorapatite: Part III. Structural characterization of sub-ppm-level Gd and Mn in minerals at W-band frequency. Am Mineral (in press)

Pan Y, Fleet MA, Chen N, Weil JA (2002b) Site preference of Gd in synthetic fluorapatite by single-crystal W-band EPR and X-ray refinement of structure: A comparative study. Can Mineral 40 (in press)

Pan Y, Fleet ME (1996a) Intrinsic and external controls on rare earth elements in calc-silicate minerals. Can Mineral 34:147-159

Pan Y, Fleet ME (1996b) Rare-earth element mobility during prograde granulite-facies metamorphism: significance of fluorine. Contrib Mineral Petrol 123:251-262

Pan Y, Stauffer MR (2000) Cerium anomaly and Th/U fractionation in the 1.85-Ga Flin Flon paleosol: Clues from accessory minerals and implications for paleoatmospheric reconstruction. Am Mineral 85:898-911

Pascher F (1963) Untersuchungen über die Austausch-barkeit des phosphors durch chrom, selen, molybdän, wolfram, und titan im apatitgitter. Tech Wiss Abhandl Osram 8:67-77

Paster TP, Schauwecker DS, Haskin LA (1974) The behaviour of some trace elements during solidification of the Skaergaard layered intrusion. Geochim Cosmochim Acta 38:1549-1577

Patel PN (1980) Magnesium calcium hydroxylapatite solid solutions. J Inorg Nuclear Chem 42:1129-1132

Pekov IV, Kulikova IM, Kabalov YuK, Yeletskaya OV, Chukanov NV, Men'shikov YuP, Khomyakov AP (1996) Belovite-(La), $Sr_3Na(La,Ce)(PO_4)_3(F,OH)$, a new rare earth mineral in the apatite group. Zap Vser Mineral Obsh 125:101-109

Peng GY, Juhr JF, McGee JJ (1997) Factors controlling sulfur concentrations in volcanic apatite. Am Mineral 82:1210-1224

Perret R, Bouillet AM (1975) The sulfate apatites $Na_3Cd_2(SO_4)_3Cl$ and $Na_3Pb_2(SO_4)_3Cl$. Bull Soc fr Minéral Cristallogr 98:254-255

Persiel E-A, Blanc P, Ohnenstetter D (2000) As-bearing fluorapatite in manganiferous deposits from St. Marcel-Praborna, Val d'Aosta, Italy. Can Mineral 38:101-117

Piriou B, Fahmi D, Dexpert-Ghys J, Taïtaï A, Lacout JL (1987) Unusual fluorescent properties of Eu^{3+} in oxyapatites. J Lumines 39:97-103

Portnov AM, Sidorenko GA, Dubinchuk VT, Kunetsova NN, Ziborova TA (1969) Melanocerite from the northern Baikal region. Doklad Akad Nauk SSSR, 185:901-904

Prener JS (1967) The growth and crystallographic properties of calcium fluor- and chlorapatite crystals. J Electrochem Soc 114:77-83

Pushcharovskii DYu, Nadezhina TN, Khomyakov AP (1987) Crystal structure of strontium apatite from Khibiny. Soviet Phys Crystallogr 32:524-526

Rakovan J, Reeder RJ (1994) Differential incorporation of trace elements and dissymmetrization in apatite: The role of surface structure during growth. Am Mineral 79:892-903

Rakovan J, Reeder RJ (1996) Intracrystalline rare earth element distributions in apatite: surface structural influences on incorporation during growth. Geochim Cosmochim Acta 60:4435-4445

Rakovan J, Hughes JM (2000) Strontium in the apatite structure: strontian fluorapatite and belovite-(Ce). Can Mineral 38:839-845

Rakovan J, Reeder RJ, Elzinga EJ, Cherniak DJ, Tait CD, Morris DE (2002) Structural characterization of U(VI) in apatite by X-ray absorption spectroscopy. Environ Sci Technol 36:3114-3117

Rakovan J, Newville M, Sutton S (2001) Evidence for heterovalent europium in zoned Llallagua apatite using wavelength dispersive XANES. Am Mineral 86:697-700

Regnier P, Lasaga AC, Berner RA, Han OH, Zilm KW (1994) Mechanism of CO_3^{2-} substitution in carbonate-fluorapatite: evidence from FTIR spectroscopy, ^{13}C NMR and quantum mechanical calculations. Am Mineral 79:809-818

Rey C, Trombe J-C, Montel G (1978a) Some features of the incorporation of oxygen in different oxidation states in the apatite lattice: III. Synthesis and properties of some oxygenated apatites. J Inorg Nuclear Chem 40:27-30

Rey C, Trombe J-C, Montel G (1978b) Sur la fixation de la glycine dans le réseau des phosphates à structure d'apatite. J Chem Res 188:2401-2416

Rey C, Collins B, Goehl T, Dickson IR, Glimcher MJ (1989) The carbonate environment in bone mineral: A resolution-enhanced Fourier transform infrared spectroscopy study. Calcif Tissue Intl 45:157-164

Roeder PL, MacArthur D, Ma XP, Palmer GR (1987) Cathodoluminescence and microprobe study of rare-earth elements in apatites. Am Mineral 72:801-811

Rønsbo JG (1989) Coupled substitution involving REEs and Na and Si in apatites in alkaline rocks from the Illimaussaq intrusions, South Greenland, and the petrological implications. Am Mineral 74:896-901

Rouse RC, Dunn PJ (1982) A contribution to the crystal chemistry of ellestadite and the silicate sulfate apatites. Am Mineral 67:90-96

Rouse RC, Dunn PJ, Peacor DR (1984) Hedyphane from Franklin, New Jersey and Laangban, Sweden; cation ordering in an arsenate apatite. Am Mineral 69:920-927

Roux P, Bonel G (1977) Sur la preparation de l'apatite carbonatée de type A, à haute température par évolution, sous pression de gaz carbonique, des arséniates tricalcique et tristrontique. Ann Chim, p 159-165

Roy DM, Drafall LE, Roy R (1978) Crystal chemistry, crystal growth, and phase equilibria of apatites. *In* Phase Diagrams, Material Sciences and Technology 6-V. Alper AM (ed) Academic Press, New York, p 186-239

Ruszala F, Kostiner E (1975) Preparation and characterization of single crystals in the apatite system $Ca_{10}(PO_4)_6(Cl,OH)_2$. J Crystal Growth 30:93-95

Ryan FM, Hopkins RH, Warren RW (1972) The optical properties of divalent manganese in strontium fluorophosphate: a comparison with calcium fluorophosphate. J Lumines 5:313-333

Schneider W (1967) Caracolit, das $Na_3Pb_2(SO_4)_3Cl$ mit apatitstruktur. N Jahrb Mineral Monatsh 284-289

Schriewer MS, Jeitschko W (1993) Preparation and crystal structure of the isotypic orthorhombic strontium perrhenate halides $Sr_5(ReO_5)_3X$ (X = chloride, bromide, iodide) and structure refinement of the related hexagonal apatite-like compound barium perrhenate chloride $(Ba_5(ReO_5)_3Cl)$. J Solid State Chem 107:1-17

Schroeder LW, Mathew M (1978) Cation ordering in $Ca_2La_8(SiO_4)_6O_2$. J Solid State Chem 26:383-387

Schwarz H (1967a) Apatite des typs $Pb_6K_4(X^VO_4)_4(X^{VI}O_4)_2$ (X^V = P,As; X^{VI} = S, Se). Z Anorg Allgem Chem 356:29-35

Schwarz H (1967b) Apatite des typs $M^{II}_{10}(X^{VI}O_4)_3(X^{IV}O_4)_3$ (M^{II} = Sr,Pb; X^{VI} = S, Cr; X^{IV} = Si ,Ge). Z Anorg Allgem Chem 356:36-45

Schwarz H (1968) Strontiumapatite des typs $Sr_{10}(PO_4)_4(X^{IV}O_4)_2$ (X^{IV} = Si ,Ge). Z Anorg Allgem Chem 357: 43-53

Serret A, Cabañas MV, Vallet-Regí M (2000) Stabilization of calcium oxyapatites with lanthanum(III)-created anionic vacancies. Chem Mater 12:3836-3841

Sery A, Manceau A, Greaves GN (1996) Chemical state of Cd in apatite phosphate ores as determined by EXAFS spectroscopy. Am Mineral 81:864-873

Simpson DR (1968) Substitutions in apatite: I. Potassium-bearing apatite. Am Mineral 53:432-444

Smith GFH, Prior GT (1911) On fermorite, a new arsenate and phosphate of lime and strontia, and tilasite, from the manganese ore deposit of India. Mineral Mag 16:84-96

Sommerauer T, Katz-Lehnert K (1985) A new partial substitution mechanism of CO_3^{2-}/CO_3OH^{3-} and SiO_4^{4-} for PO_4^{3-} group in hydroxy-apatite from the Kaiserstuhl alkaline complex. Contrib Mineral Petrol 91:360-368

Soules TF, Davis TS, Kreidler ER (1971) Molecular orbital model for antimony luminescent centers in fluorophosphates. J Chem Phys 55:1056-1064

Steele IM, Pluth JJ, Livingstone A (2000) Crystal structure of mattheddleite, a Pb, S, Si phase with the apatite structure. Mineral Mag 64:915-921

Steinbruegge KB, Henningsen T, Hopkins RH, Mazelsky R, Melamed NT, Riedel EP, Roland DW (1972) Laser properties of Nd^{+3} and Ho^{+3} doped crystals with the apatite structure. Appl Optics 11:999-1012

Sudarsanan K (1980) Structure of hydroxylellestadite. Acta Crystallogr B36:1636-1639

Sudarsanan K, Mackie PE, Young RA (1972) Comparison of synthetic and mineral fluorapatite, $Ca_5(PO_4)_3F$, in crystallographic detail. Mater Res Bull 7:1331-1338

Sudarsanan K, Young RA (1974) Structure refinement and random error analysis for strontium "chlorapatite", $Sr_5(PO_4)_3Cl$. Acta Crystallogr B30:1381-1386

Sudarsanan K, Young RA (1980) Structure of partially substituted chlorapatite $(Ca,Sr)_5(PO_4)_3Cl$. Acta Crystallogr B36:1525-1530

Sudarsanan K, Young RA, Wilson AJC (1977) The structures of some cadmium "apatites" $Cd_5(MO_4)_3X$: I. Determination of the structures of $Cd_5(VO_4)_3I$, $Cd_5(PO_4)_3Br$, $Cd_5(AsO_4)_3Br$ and $Cd_5(VO_4)_3Br$. Acta Crystallogr B33:3136-3142

Suetsugu Y, Takahashi Y, Okamura FP, Tanaka J (2000) Structure analysis of A-type carbonate apatite by a single-crystal X-ray diffraction method. J Solid State Chem 155:292-297

Suitch PR, Lacout JL, Hewat A, Young RA (1985) The structural location and role of Mn^{2+} partially substituted for Ca^{2+} in fluorapatite. Acta Crystallogr B41:173-179

Suitch PR, Taïtaï A, Lacout JL, Young RA (1986) Structural consequences of the coupled substitution of Eu, S, in calcium sulfoapatite. J Solid State Chem 63:267-277

Taïtaï A, Lacout JL (1989) On the coupled introduction of Eu^{3+} and S^{2+} ions into strontium apatites. J Phys Chem Solids 50:851-855

Takahashi M, Uematsu K, Ye ZG, Sato M (1998) Single-crystal growth and structure determination of a new oxide apatite, $NaLa_9(GeO_4)_6O_2$. J Solid State Chem 139:304-309

Terpstra RA, Driessens FCM (1986) Magnesium in tooth enamel and synthetic apatites. Calcif Tissue Intl 39:348-354

Tochon-Danguy HT, Very JM, Geoffroy M, Baud CA (1978) Paramagnetic and crystallographic effects of low temperature ashing on human bones and tooth enamel. Calcif Tissue Intl 25:99-104

Trombe J-C, Montel G (1975) Sur les conditions de préparation d'une nouvelle apatite contenant des ions sulfure. Compt Rend Acad Sci 280:567-570

Trombe J-C, Montel G (1978) Some features of the incorporation of oxygen in different oxidation states in the apatite lattice-II. On the synthesis and properties of calcium and strontium peroxiapatites. J Inorg Nuclear Chem 40:23-26

Trombe J-C, Montel G (1981) On the existence of bivalent ions in the apatite channels. A new example-phosphocalcium cyanamido-apatite. J Solid State Chem 40:152-160

Trueman NA (1966) Substitutions for phosphate ions in apatite. Nature 210:937-938

Urusov VS, Khudolozhkin VO (1974) An energy analysis of cation ordering in apatite. Geochem Intl 11:1048-1053

Vali H, McKee MD, Ciftcioglu N, Sears SK, Plows FL, Chevet E, Ghiabi P, Plavsic M, Kalander EO, Zare RN (2001) Nanoforms; a new type of protein-associated mineralization. Geochim Cosmochim Acta 65: 63-74

Verbeeck RMH, Lassuyt CJ, Heijligers HJM, Driessens FCM, Vrolijk JWGA (1981) Lattice parameters and cation distribution of solid solutions of calcium and lead hydroxyapatites. Calcif Tissue Intl 33:243-247

Vignoles M, Bonel G (1978) Sur la localisation des ions fluorure dans les carbonate-apatites de type B. Compt Rend Acad Sci 287:321-324

Vignoles M, Bonel G, Young RA (1987) Occurrence of nitrogenous species in precipitated B-type carbonated hydroxyapatites. Calcif Tissue Intl 40:64-70

Wallaeys R (1952) Contribution à l'étude des apatites phosphocalciques. Ann Chim 7:808-848

Warren RW (1970) EPR of Mn^{+2} in calcium fluorophosphate: I. The Ca(II) site. Phys Rev B2:4383-4388

Warren RW (1972) Defect centres in calcium fluorophosphate. Phys Rev B6:4679-4689

Warren RW, Mazelsky R (1974) EPR of Mn^{+2} in calcium fluorophosphate. II. Modified Ca(II) site. Phys Rev B10:19-25

Watson EB (1976) Two-liquid partition coefficients: Experimental data and geochemical implications. Contribut Mineral Petrol 56:119-134

Watson EB, Green TH (1981) Apatite/liquid partition coefficients for the rare earth elements and strontium. Earth Planet Sci Lett 56:405-421

Watson EB, Harrison TM, Ryerson FJ (1985) Diffusion of Sm, Sr, and Pb in fluorapatite. Geochim Cosmochim Acta 49:1813-1823

Welin E (1968) X-ray powder data for minerals from Långban and the related mineral deposits of Central Sweden. Arkiv Mineral Geol 4:499-541

Wilson AJC, Sudarsanan K, Young RA (1977) The structures of some cadmium "apatites" $Cd_5(MO_4)_3X$: II. The distribution of the halogen atoms in $Cd_5(VO_4)_3I$, $Cd_5(PO_4)_3Br$, $Cd_5(AsO_4)_3Br$ and $Cd_5(VO_4)_3Br$. Acta Crystallogr B33:3142-3154

Wilson RM, Elliott JC, Dowker SEP (1999) Rietveld refinement of the crystallographic structure of human dental enamel apatites. Am Mineral 84:1406-1414

Wondratschek H (1963) Untersuchungen zur kristallchmie der blei-apatite (pyromorphite). N Jahrb Mineral Abh 99:113-160

Wright J, Seymour RS, Shaw HF (1984) REE and neodymium isotopes in conodont apatite: Variations with geological age and depositional environment. Geol Soc Am Spec Pap 196:325-340

Wronkiewicz DJ, Wolf SF, Disanto TS (1996) Apatite- and monazite-bearing glass-crystal compositions for the immobilization of low-level nuclear and hazardous wastes. Mater Res Soc 412:345-352

Young EJ, Munson EL (1966) Fluor-chlor-oxy-apatite and sphene from Crystal Lode pegmatite near Eagle, Colorado. Am Mineral 51:1476-1493

Young EJ, Myers AT, Munson EL, Conklin NM (1969) Mineralogy and geochemistry of fluorapatite from Cerro de Mercado, Durango, Mexico. U S Geol Surv Paper 650-D:84-93

Zhang JH, Fang Z, Liao LB (1992) A study of crystal structure of britholite-Y. Acta Mineral Sinica 12: 132-142 (in Chinese).